Wt1-expressing cells contribute to mesoderm-derived tissues in intestine and mesentery in two distinct phases during murine embryonic development.

Suad Alghamdi[$1], Thomas P Wilm[$1], Shanthi Beglinger[1], Michael Boyes[1], Helen Tanton[1,3], Fiona Mutter[1], Joanna Allardyce[1,4], Veronica Foisor[1,5], Ben Middlehurst[1], Lauren Carr[1], Kelly Ward[1], Tarek Benameur[1,6], Thomas Butts[1], Nicholas Hastie[2], Bettina Wilm[1^]

[$] contributed equally

Affiliation:

1 Department of Molecular Physiology and Cell Signalling, Institute of Systems, Molecular and Integrative Biology, University of Liverpool, Liverpool, UK

2 MRC Human Genetics Unit, University of Edinburgh, Edinburgh, UK

3 present address: Department of Oncologic Pathology, Dana-Farber Cancer Institute, Harvard Medical School, Boston, USA

4 present address: School of Allied Health, Education and Health Sciences, University of Limerick, Limerick, Ireland

5 present address: Department of Chemistry, University of Warwick, Coventry, UK

6 present address: College of Medicine, Department of Biomedical Sciences, King Faisal University, Al Ahsa, Kingdom of Saudi Arabia

ORCIDs:

HT 0000-0002-0129-5870

VF 0000-0001-7004-1324

NH 0000-0002-0515-168X

BW 0000-0002-9245-993X

^ Corresponding author:

b.wilm@liverpool.ac.uk

Abstract

The mesoderm gives rise to diverse tissues including the mesothelium, as well as the visceral and vascular smooth muscle. Previously, genetic lineage tracing based on the mesothelial marker Wt1, appeared to show that visceral mesothelial cells are the direct progenitors of vascular smooth muscle in the intestine. However, the timing and underlying developmental mechanisms regulating this lineage were not fully understood. Here, using a temporally-controlled Wt1-based genetic lineage tracing approach, we demonstrate that (i) the adult visceral mesothelium of the intestine only maintains itself and fails to contribute to other visceral tissues; (ii) the vascular and visceral smooth muscle in the developing intestine and mesentery arise earlier than and independently from the visceral mesothelium. Our results suggest that Wt1 is switched on and remains expressed in the visceral mesothelium from around E9.5 onwards throughout life, while earlier transient expression of Wt1 in the nascent mesoderm specifies the future vascular and visceral smooth muscle of intestine and mesentery.

Keywords: mesothelium, Wilms tumour protein 1, genetic lineage tracing, tamoxifen, tissue homeostasis, embryonic development, smooth muscle cells, light sheet microscopy, mouse

Introduction

During embryonic development, vascular smooth muscle cells (VSMCs) and pericytes arise from different sources, including the neural crest, the somatic and the lateral plate mesoderm (Majesky, 2018, Roostalu and Wong, 2018, Wang et al., 2015). Hence, VSMCs / pericytes appear to form a mosaic with different developmental origins (Bentzon and Majesky, 2018). Recently, the molecular mechanisms by which VSMCs or pericytes differentiate from induced pluripotent stem (iPS) cells in vitro have been described (Kumar et al., 2017), however, it remains unclear how VSMCs or pericytes are specified or recruited in vivo to the developing vasculature.

The epicardium, the mesothelium of the heart, contributes VSMCs to the developing coronary vessels (Red-Horse et al., 2010, Zhou et al., 2008). Based on this observation, we previously tested the hypothesis that a similar developmental relationship exists between the visceral mesothelium and the vasculature of the intestine. The visceral mesothelium of the peritoneal cavity arises from the lateral plate mesoderm, where it forms a simple squamous epithelium covering all organs within the cavity (Wilm et al., 2005, Winters et al., 2012). The Wilms' tumour protein 1 (Wt1) is a key marker of mesothelia, and a transgenic mouse line expressing Cre recombinase under control of regulatory elements of the human WT1 gene (Tg(WT1-cre)AG11Dbdr, in short: Wt1-Cre) had been previously used to track mesothelial cells in mice (Wilm et al., 2005). In adult Wt1-Cre; $Rosa26^{LacZ/LacZ}$ compound mutant mice, XGal-labelled vascular smooth muscle cells were found in the vasculature of the mesentery and intestine, as well as the heart and lungs (Que et al., 2008, Wilm et al., 2005). These findings led us to conclude that cells of the visceral mesothelium give rise directly to VSMCs in the intestine and mesentery (Wilm et al., 2005). Studies using a different Wt1-Cre line (Tg(Wt1-cre)#Jbeb) revealed a similar contribution of Wt1-expressing cells to the mesothelium and the visceral and vascular smooth muscle of the developing intestine (Carmona et al., 2013).

However, these genetic lineage tracing systems were unable to distinguish the time window during embryonic development or postnatal stages when cells had expressed Wt1, as once tagged, the cells

were consequently irreversibly labelled. Therefore, it is unclear whether Wt1-expressing mesothelial cells give rise to VSMCs continuously throughout life, or only during a specific time window in embryonic development. Furthermore, it is not clear whether postnatal or even adult mesothelial cells in the peritoneal cavity generally contribute to the maintenance of the intestinal and parietal body wall. This is pertinent because of reports suggesting that mesothelial cells have the plasticity to differentiate into cells of different mesodermal lineages (Colunga et al., 2019, Karki et al., 2014, Mutsaers et al., 2015, Dauleh et al., 2016).

To address these questions, we determined the spatio-temporal contribution of Wt1-expressing cells to the adult, postnatal and embryonic intestine and parietal peritoneum, as well as the VSMCs in the mesentery and intestinal wall. For this purpose, we used a temporally controlled and Wt1-driven Cre system ($Wt1^{tm2(cre/ERT2)Wtp}$) which relies on tamoxifen administration to activate recombination and thus lineage tracing (Wilm and Munoz-Chapuli, 2016, Zhou et al., 2008). Our analysis revealed that Wt1-lineage traced mesothelial cells in neonatal or adult intestine and peritoneal body wall only contributed to maintenance of cells of the serosa (and mesenteric fat) and not to vascular cells or intestinal wall tissue. This was different in the heart, where coronary vasculature was labeled, indicating postnatal epicardial contribution. By contrast, Wt1-lineage tracing in the embryo indicated two stages of contribution: (i) Wt1-expressing cells solely gave rise to the visceral mesothelium of intestine and mesentery from around E9.5 onwards; and (ii) Wt1-expressing cells labeled at between E7.5 and E8.5 contributed to vascular and visceral smooth muscle cells in the intestine and mesentery in spatially restricted segments. Thus, our analysis describes two separate phases of lateral mesoderm differentiation which contribute to different lineages and indicates that Wt1 plays separate roles within each. Our data for the first time delineate the temporal events that lead to vascular and visceral smooth muscle cell formation and separately to visceral mesothelium development in the intestine and mesentery.

Results

Adult Wt1-derived cells contribute to coronary but not intestinal vascular cells and maintain the visceral and parietal mesothelium

We examined whether mesothelial cells (MCs) contribute to the formation of vascular cells and other tissue components in the adult intestine. After a 2-4 week chase period in $Wt1^{CreERT2/+}$; $Rosa26^{LacZ/LacZ}$ and $Wt1^{CreERT2/+}$; $Rosa26^{mTmG/+}$ mice we found lineage-traced cells in a patchy pattern in the intestinal serosa (Figure 1A, B). In addition, we observed a recently described Wt1-expressing submesothelial mesenchymal population (Buechler et al., 2019) in the serosa of the mesentery and body wall, and in the omentum (Supplementary Figure S1). We could not detect any contribution of labelled Wt1-expressing mesothelial cells to vascular smooth muscle in the mesentery or the intestine, or other cell types of body or intestinal wall, except for the previously reported contribution to mesenteric fat, which was confirmed by histological analysis (Figure 1E, F, Supplementary Figure S2A, B) (Chau et al., 2014, Chau et al., 2011). Both the $Wt1^{CreERT2/+}$; $Rosa26^{LacZ/LacZ}$ and $Wt1^{CreERT2/+}$; $Rosa26^{mTmG/+}$ reporter systems gave very similar results, as revealed by direct comparison of GFP and XGal staining in the intestinal mesothelium in $Wt1^{CreERT2/+}$; $Rosa26^{LacZ/mTmG}$ mice (Supplementary Figure S3).

To determine whether the previously reported contribution of MCs to the intestinal vascular smooth muscle compartment is controlled by a slow process of tissue homeostasis, we performed a long-term chase experiment of two and six months, respectively. Our data revealed that even six months after the tamoxifen pulse, coverage of the visceral mesothelium with labelled cells was still patchy, and no contribution to intestinal vascular smooth muscle cells could be detected (Supplementary Figure 4). Furthermore, using the $Wt1^{CreERT2/+}$; $Rosa26^{Confetti/+}$ reporter system, we observed a limited clonal expansion of labelled visceral MCs in adult mice over time (Supplementary Figure S5). Therefore, our observations indicate that MCs in healthy adult mice were restricted to maintaining homeostasis of the peritoneum at a low turnover rate (Mutsaers, 2004).

To test this observation further we ablated Wt1 in adult mesothelial cells by using $Wt1^{CreERT2/co}$ mice, similar to the approach described by Chau and colleagues (Chau et al., 2011). We observed severely deteriorating health in all animals from approximately day 10 after the start of tamoxifen administration onwards, as described (Chau et al., 2011). This precluded a detailed analysis of the impact of loss of Wt1 on the homeostasis of the serosa of the peritoneum and in particular the intestine. However, our histological analysis of various regions of the intestine at day 10 after tamoxifen administration showed no effect on the presence and appearance of the mesothelium, or the overall intestinal morphology (Supplementary Figure S6).

Lineage-traced epicardial cells were found in patches over the heart in adult mice (Figure 1C, D, Supplementary Figure S2C), but also formed part of the coronary vasculature of the heart even after a 2-week chase period (Figure 1C', Supplementary Figure S2D). The coronary contribution was more difficult to determine in whole mount tissue analysis of mice carrying the $Wt1^{CreERT2/+}$; $Rosa26^{mTmG/+}$ reporter because of the strong coverage of GFP-expressing cells in the epicardium (Figure 1D'). Histological analysis of the heart wall showed that Wt1-derived GFP^{+} cells localised around coronary vessels and co-expressed the classical vascular smooth muscle cell marker α-smooth muscle actin (SMA), or the endothelial marker CD31 (Figure 1G, H), in line with reports showing that epicardial cells can contribute to the endothelial and mural component of the coronary vessels (Red-Horse et al., 2010, Zhou et al., 2008, Wilm et al., 2005).

We also included kidneys in our analysis because adult podocytes express Wt1, thus allowing assessment of successful tamoxifen administration. Adult kidneys showed the expected labelling of glomeruli two weeks after tamoxifen (Supplementary Figure S7A-D), where GFP-positive cells co-expressed Wt1, indicating their podocyte identity (Supplementary Figure S7D). We occasionally (1 out of 10 analysed kidneys) observed one or two XGal- or GFP-labelled tubules in the medulla region of the sagittally dissected kidneys (Supplementary Figure S7E and for GFP not shown), suggesting that there was a small population of Wt1-expressing cells in the adult kidney with the potential to contribute to the tubular elements of the nephrons.

Wt1-derived cells in newborn lineage tracing reveal wider contribution to the heart and kidneys, but not to the serosal mesothelium

Since the adult serosa of the peritoneum appeared to be restricted to its maintenance, we tested whether mesothelial cells may still have some degree of plasticity either in juvenile mice directly after weaning, or within the first few days after birth (Boulland et al., 2013, Hartman et al., 2007, Porrello and Olson, 2014, Seely, 2017), and thus would show capacity to contribute to intestinal tissue homeostasis or to differentiate into VSMCs. After tamoxifen administration in four weeks old juvenile $Wt1^{CreERT2/+}$; $Rosa26^{LacZ/+}$ mice and chase periods between 7 and 17 weeks, restricted contributions of Wt1-derived XGal-stained cells were found in similar locations to those in adult mice (data not shown). Correspondingly, after initiating a 7-weeks chase period in newborn $Wt1^{CreERT2/+}$; $Rosa26^{LacZ/+}$ mice, we detected coverage of XGal-stained cells in the visceral mesothelium comparable to adult mice (Figure 2A), and no contribution to the vasculature of the mesentery or intestine, or within the intestinal wall (Figure 2B, C). By contrast, lineage-traced cells were found as expected in the epicardial layer of the heart, and also contributing to its coronary and micro-vasculature (Figure 2D-F). These results indicate that while in the newborn, Wt1-expressing epicardial cells continued to give rise to coronary vessels, visceral mesothelial cells failed to contribute to the intestinal vasculature (Porrello and Olson, 2014, Cao and Poss, 2018, Porrello et al., 2011, Quijada et al., 2020).

In the kidneys, neonate Wt1-expressing cells gave rise to XGal-stained cells in the glomeruli and in nephron tubules (Figure 2G-J). In contrast to lineage tracing in adult kidneys, the contribution of XGal-labelled cells to the nephron tubules was abundant, indicating that Wt1-expressing cells in the neonatal kidneys still had the capacity to give rise to entire nephron structures (Hartman et al., 2007).

Taken together, our lineage tracing analysis of newborn, juvenile and adult mice showed that Wt1-expressing cells of the peritoneum failed to contribute to the vasculature, or other components of

the intestinal or body wall besides mesenteric fat. This indicates that in healthy postnatal mice peritoneal mesothelial cells are mostly restricted to self-renewal.

From E9.5 onwards, Wt1-expressing cells give rise to visceral mesothelium

Next, we aimed to determine at which time point of prenatal development Wt1-expressing cells gave rise to intestinal vascular smooth muscle. We administered tamoxifen once to time-mated pregnant females at stages between E14.5 and E7.5, followed by analysis just before birth (Figure 3, Supplementary Table 1). Whole mount analysis for LacZ staining or GFP fluorescence in intestine and mesentery revealed that after tamoxifen administration at stages between E10.5 and E14.5, Wt1-expressing cells contributed solely to the mesothelium (Figure 3A-C, Supplementary Figure S8B, E, H, J, K and data not shown). We noted that the coverage of the mesothelium of the intestine and mesentery with LacZ-positive lineage-traced cells was almost complete when tamoxifen had been administered at stages E13.5 and E12.5 (Figure 3A, B), while tamoxifen given at stages E14.5, E11.5, E10.5 or E9.5 led to a more patchy distribution of XGal-stained or GFP-labelled cells in the mesenteric and intestinal mesothelium (Figure 3C, D, Supplementary Figure S8B, E, H, H', J, J', K, and data not shown). We also observed that activation of the Wt1-based lineage tracing in the mesothelium at these stages resulted in the presence of labeled cells along the entire length of the small intestine (Supplementary Figure S8B). Immunostaining of tissue sections of $Wt1^{CreERT2/+}$; $Rosa26^{mTmG/+}$ embryos after tamoxifen administration at E11.5 and analysis at E19.5 confirmed that the presence of the GFP-labelled cells was limited to the visceral mesothelium, where these cells co-expressed cytokeratin and Wt1 (Figure 4A, A', B, B'). By contrast, we failed to observe any co-expression of GFP with the endothelial marker CD31 or the vascular smooth muscle marker SMA within the intestine or mesentery at these stages (Figure 4C, C', D, D').

Between E7.5 and E8.5, Wt1-expressing cells give rise to visceral and vascular smooth muscle of the intestine

When we administered tamoxifen at E7.5 and analysed the embryonic intestines just before birth, labelled cells were found as vascular smooth muscle cells in short segments of the mesenteric vasculature (Figure 3I). Within these regions, labelled cells were also scattered within the mesentery (Figure 3G). Similarly, after tamoxifen administration at E8.5, we found that XGal-positive cells contributed consistently to vascular smooth muscle cells in short segments of the mesenteric vasculature, but also to small patches of the mesothelium over the mesentery (Figure 3E, F, Supplementary Figure S8I, L, Supplementary Table 1). In addition, after tamoxifen administration at both E8.5 and E7.5, labelled cells were found as circular visceral smooth muscle in discreet segments of the small intestine (Figure 3H, Supplementary Figure S8C, F, G, I, M). In embryos of one litter after Tamoxifen at E9.5 and analysis before birth we observed the presence of a few labelled vascular and visceral smooth muscle cells, while in a second litter with identical treatment, these labelled cells were not detectable (Supplementary Table 1 and data not shown), suggesting a very narrow time window of deciding the potential developmental fate.

Immunostaining of tissue sections from $Wt1^{CreERT2/+}$; $Rosa26^{mTmG/+}$ embryos after tamoxifen at E8.5 and analysis at E17.5 showed that GFP-positive cells co-expressed SMA but not CD31 in mesenteric blood vessels (Figure 4G, G', H, H'). Furthermore, GFP-labelled cells were positive for SMA in the visceral smooth muscle (Figure 4I, I'). A few Wt1-expressing mesothelial cells in the mesentery were also GFP-positive (Figure 4F, F').

These results suggest that Wt1-expressing cells gave rise to some of the visceral mesothelium covering the mesentery and intestine from E8.5 onwards. However, already in E7.5 embryos, before mesothelium formation, Wt1-expressing cells were the source of vascular and visceral smooth muscle of the intestine and mesentery, indicating that the visceral and vascular smooth muscle cells arise independently of mesothelium formation. Of note, our data suggest that there is a developmental overlap between these separate lineages at around E8.5 to E9.5.

We performed whole mount in situ hybridisation for *Wt1* of mouse embryos between E7.5 and E9.5, to determine which expression domain would correspond to the activation of Cre recombinase and resultant lineage tracing at the observed stages (Supplementary Figure 9). Our analysis showed that there was relatively high unspecific background staining in embryos between E7.5 and E8.5, with faint signals in the posterior of the embryos near the primitive streak (Supplementary Figure 9A, C). By contrast, at E9.0-E9.5 the previously described domains in the epicardium and the urogenital ridge were clearly detectable (Supplementary Figure S9E, F) (Armstrong et al., 1993).

Tracking lineage-labelled cells during embryonic stages reveals their fate

In order to gain further understanding of the characteristics and fate of the lineage labeled cells, we administered tamoxifen at E7.5 or E8.5 and analysed the embryos at E9.5. Tamoxifen administration at E7.5 revealed GFP expression in a discreet population of around 7-9 epicardial cells in the E9.5 embryo (Figure 5A-C). In addition, in a total of three litters, we also observed four embryos with small groups of GFP-expressing cells in the neural tube at the level of heart or liver formation (Supplementary Figure S10 and data not shown). By contrast, tamoxifen administration at E8.5 followed by analysis at E9.5, showed GFP-expressing cells in both the epicardium and the region encompassing the intermediate/lateral mesoderm (Figure 5D-H). Importantly, immunofluorescence analysis of sections and light sheet microscopy demonstrated individual GFP-positive cells within the region between the intermediate mesoderm and the mesentery, and in close vicinity to the dorsal aorta, suggesting a functional role of these cells in this tissue (Figure 5 G, H, Movies 1, 2). Light sheet microscopy further revealed GFP-positive cells in the lateral plate and intermediate mesoderm and in the mesentery, but also in the neural tube (Movie 1, Supplementary Figure S11).

We next administered tamoxifen to embryos at E8.5 and performed analysis at later stages, which revealed a dynamic pattern of GFP-expressing cells (Supplementary Figure S12). Whole mount analysis at E10.5 (after tamoxifen administered at E8.5), showed prominent GFP-expressing cells in

the heart and urogenital ridge, but also in an isolated speckled appearance in other regions of the embryo (Supplementary Figure S12A). In sections through levels below the heart, we detected a number of GFP-expressing cells in the urogenital ridge, but also in the region between the dorsal aorta and the mesentery (Supplementary Figure S12B). Analysis at E12.5 showed GFP-expressing cells in the mesentery of the developing intestine (Supplementary Figure S12C, C'), which were also localised near the developing endothelial plexus in the mesentery and intestinal wall (Supplementary Figure S12D, F), and co-expressed the mesenchymal marker PDGFRβ (Supplementary Figure S12E-E''). Of note, we observed abundant GFP-expressing cells in the liver (Supplementary Figure S12C, C'). At E15.5, small segments of intestine contained GFP-expressing cells, some of which had already taken up appearance of circular visceral smooth muscle (Supplementary Figure S12G, H). These observations suggest that the Wt1-derived cells descended from non-mesothelial cells and moved as mesenchymal cells via the mesentery to the intestine while adopting their vascular and visceral smooth muscle fate.

Taken together, our results indicate that cells expressing Wt1 predominantly between E7.5 and E8.5 contributed to vascular and visceral smooth muscle formation in the developing small intestine and mesentery. This process was clearly independent of the establishment of the mesothelium of the intestine and parietal peritoneum from around E9.5 onwards, by an as yet unknown developmental mechanism. Further studies are needed to elucidate the molecular mechanisms that drive the development of Wt1-expressing cells in the gastrulating embryo towards vascular and visceral smooth muscle fate, and the role of Wt1 during this process.

Discussion

Here, we have attempted to dissect the relationship between Wt1 expression and the mesothelial lineage with particular focus on the embryonic development of the visceral and vascular smooth

muscle in the intestine and mesentery. By utilising temporally controlled lineage tracing of Wt1-expressing cells, our results have revealed that the formation of the peritoneal mesothelium and the visceral and vascular smooth muscle of intestine and mesentery, are linked to Wt1 expression, but in two distinct phases. Wt1-based lineage tracing in the embryo and in postnatal stages has shown that once the mesothelium of intestine and mesentery has formed from around E9.5 onwards, this tissue maintains itself, and fails to contribute to other tissues except visceral fat. By contrast, in an earlier phase, Wt1-expressing cells present in the embryo predominantly between E7.5 and E8.5 and not later than E9.5, give rise to the visceral and vascular smooth muscle of the intestine and mesentery. Therefore, our findings presented here indicate two phases of contribution of Wt1-expressing cells to mesodermal tissues in the peritoneal cavity.

The mesothelium is a continuous sheet covering the organs housed within the three body cavities, pleural, pericardial and peritoneal, and lining the walls of the cavities. Our previous study, using a continuously active Cre only controlled by the human WT1 promoter, had shown that Wt1-expressing cells contributed to the vasculature of the mesentery and intestine (Wilm et al., 2005). Based on this finding we concluded that the visceral mesothelium gives rise to these vascular structures during embryonic development. Further, our results led us to hypothesise that there may be a role for the visceral mesothelium in maintaining the vasculature, and possibly other intestinal structures during adult life. The work presented here, using a temporally-controlled tamoxifen-inducible reporter system driven from the endogenous Wt1 locus, demonstrates that the relationship between Wt1 expression and mesothelial lineage is more complex. In particular, we have shown here that the adult serosa of the peritoneal cavity, only maintains itself, besides giving rise to visceral fat.

Previous pulse-chase studies using the same tamoxifen-inducible Wt1-driven reporter system as used in this report, had shown that the postnatal lung mesothelium makes no contribution to other cells within the lungs (von Gise et al., 2016). By contrast, embryonic lineage tracing experiments

revealed that the Wt1-expressing lung mesothelium at E10.5 gives rise to bronchial and vascular smooth muscle, as well as PDGFRβ-expressing pericytes and PDGFRα-expressing fibroblasts (von Gise et al., 2016).

In the liver, the visceral mesothelium arises from the septum transversum at around E9.0. Wt1 is expressed in the septum transversum, and later in the liver mesothelium from E11.5 onwards and throughout postnatal stages (Asahina et al., 2011). Using the tamoxifen-inducible Wt1-based lineage tracing system during embryonic development of the liver mesothelium demonstrated that mesothelial cells give rise to submesothelial cells, hepatic stellate cells as well as perivascular mesenchymal cells, while lineage tracing in the adult liver revealed that only the visceral Wt1-expressing mesothelium is labeled (Asahina et al., 2011, Lua et al., 2015).

Previously, Lua and colleagues had demonstrated that parietal mesothelial cells have a different developmental origin compared to the liver mesothelium, using a Mesp1-Cre-based lineage system (Lua et al., 2015, Asahina et al., 2009). However, the developmental origin of the parietal mesothelium has not been further assessed. Lineage tracing of the adult parietal mesothelium of the peritoneal cavity using the tamoxifen-inducible Wt1-based lineage system revealed self-maintenance of the mesothelium (Lua et al., 2015), while a minor contribution to collagen 1a1-expressing submesothelial cells was observed by Chen and colleagues (Chen et al., 2014). A recent study confirmed by cytometric sorting the presence of a small population of submesothelial fibroblastic cells that expresses Wt1 together with the mesothelial marker podoplanin and the fibroblast marker PDGFRα, with a possible role in maintaining Gata6 expression in large cavity macrophages (Buechler et al., 2019). Here, we have visualized these cells using the lineage tracing system.

Our own findings suggest that during embryonic development, the visceral mesothelium of the intestine is different to that of the liver and lung since after its emergence it fails to contribute to the stroma of the intestinal wall. However, the postnatal visceral mesothelium appears to behave

similarly between the lung, liver and intestine in that there is no contribution to stromal compartments, other than the progenitor niche of the visceral fat.

During embryonic development of the heart, Wt1-expressing epicardial cells have been shown to contribute to the mural cells of the coronary vessels as well as fibroblasts (Rudat and Kispert, 2012, Sereti et al., 2018, Tian et al., 2013). In the adult heart, Wt1 expression is downregulated (Smart et al., 2011), and lineage tracing studies using the tamoxifen-inducible Wt1-driven lineage system in adult mice have revealed no contribution to cells other than the epicardium (Quijada et al., 2020, Zhou et al., 2011). Our data presented here suggest that in the adult as well as in newborns, the tamoxifen-inducible Wt1-driven lineage system allows the detection of Wt1-derived cells in the coronary endothelial and mural cells. This is particularly striking since the visceral mesothelium of the postnatal intestine failed to provide this contribution.

Of note, in contrast to the normal, healthy mesothelium, lineage tracing studies after injury in the lungs, liver, heart and peritoneum have shown that adult mesothelial cells can be activated and undergo a range of physiological changes including epithelial-mesenchymal transition (EMT) into smooth muscle cells and myofibroblasts, and subsequent contribution to scar formation (Chen et al., 2014, Karki et al., 2014, Lua et al., 2015, Namvar et al., 2018, Smart et al., 2011, Kendall et al., 2019).

In the kidneys, we observed differences in the contribution to renal tissue between adult and newborn lineage tracing, indicating that there is a larger degree of plasticity present in the newborn kidney, where Wt1-expressing cells contribute to nephron tubules in addition to the glomeruli and parietal epithelial cells of the Bowman's capsule.

It is important to point out that the efficiency of cell labelling in lineage tracing systems using the $Wt1^{CreERT2/+}$; $Rosa26^{mTmG/+}$ mouse line has been reported to be between 14.5% and 80% in different laboratories (Chen et al., 2014, Li et al., 2013), suggesting that rare lineage labelling events may not be detected using this approach (Rudat and Kispert, 2012). Therefore, in the current study, we can

conclude that XGal- or GFP-positive cells have expressed Wt1 at the time of tamoxifen administration, but there may be some cells that have expressed Wt1 which are not labelled and evade the lineage tracing system. The reasons for this variation could be inefficiency of the recombination system or insufficiency of the tamoxifen distribution inside the animals.

One of the unexpected findings in this study was the observation that Wt1-derived cells contribute to the vascular and visceral smooth muscle in the intestinal wall and mesentery before the emergence of the mesothelium. In our previous study, we had used a transgenic mouse line (*Tg(WT1-cre)AG11Dbdr*; *Gt(ROSA)26Sor*/J; in short Wt1-Cre; Rosa26^{LacZ}) composed of a Cre reporter system driven by human Wilms Tumour protein 1 (WT1) regulatory elements (Wilm et al., 2005), which had been shown to faithfully recapitulate the Wt1 expression domains in mice (Moore et al., 1998). In the Wt1-Cre; Rosa26^{LacZ} mice, XGal staining had been prominent in the vascular smooth muscle surrounding the veins and arteries in the mesentery and those inserting into the intestinal wall. We concluded that the labelled vascular smooth muscle cells, which had expressed Wt1 at some undetermined time point in the life of the mouse, must have arisen from the visceral mesothelium as the only known tissue in the peritoneal cavity to express Wt1 in the embryo and throughout life (Wilm et al., 2005). What remained unknown was the time point at which the vascular smooth muscle fate was induced in the mesothelial cells. To address this question, we performed the temporally controlled lineage study presented here. Our new data suggest that the vascular and visceral smooth muscle cells labelled in the mesentery and intestine, arise from so far undetermined Wt1-expressing cells in embryos at around E7.5 to E8.5, but not later than E9.5. Very few visceral mesothelial cells in intestine and mesentery were found to be GFP-positive after tamoxifen administration in this early developmental time window. It is important to note that there is a time lag between tamoxifen administration and onset of Cre activation and subsequent recombinatory activity in the nucleus of about 12-24 hours (Nakamura et al., 2006), suggesting that

Cre activity may be targeting Wt1-expressing cells from around E8.0 onwards when tamoxifen is administered at E7.5.

In the primitive streak mesoderm, Mesp1 has been shown to be active during gastrulation stages (E6.5-E8.0) (Saga et al., 1996). Interestingly, Asahina and colleagues found that embryonic Mesp1-Cre driven lineage tracing, via the septum transversum mesenchyme, gave rise to liver mesothelial cells as well as cells within the liver parenchyma, but not to parietal mesothelial cells (Asahina et al., 2009). Furthermore, the group demonstrated that in $Wt1^{CreERT2/+}$; $Rosa26^{mTmG}$ E11.5 embryos the entire liver mesothelium contains GFP-positive cells when tamoxifen is administered at both E7.5 and E8.5 (Asahina et al., 2011), similar to our own observation of abundant GFP-positive cells over and in the liver at E12.5 after tamoxifen at E8.5. Together with our own observations presented here, this would suggest that there are differences in the developmental mechanisms by which the visceral mesothelium of the liver and the intestine as well as the parietal mesothelium are formed.

In some of the E9.5 embryos after tamoxifen administration at E7.5, we observed the presence of GFP-positive cells within a very restricted domain of the neural tube. This is in contrast to previous reports that Wt1 expression in the neural tube starts between E11 and E12 in the mouse embryo (Armstrong et al., 1993, Haque et al., 2018). The restricted GFP domain in the neural tube suggested that these cells were Cre-recombined after tamoxifen administration while transiently expressing Wt1 and undergoing a short specific phase of gastrulation, possibly as epiblast cells. Whether Wt1 is indeed expressed in the epiblast during early gastrulation stages needs to be confirmed in future studies. However, the observation that the GFP-positive visceral and vascular smooth muscle cells within intestine and mesentery after tamoxifen administration at E7.5 or E8.5 were restricted to specific segments of the small intestine supports the interpretation that the cells originally expressed Wt1 in a short and transient phase during embryonic development.

While our findings here shed new light on the temporal processes of the development of vascular and visceral smooth muscle in the intestine and mesentery, future studies are needed to elucidate the

molecular mechanisms, in particular the role of Wt1, that drive these steps in the gastrulating embryo.

Methods

Mice

The following compound mutants were generated for this study by breeding existing mouse lines: $Wt1^{CreERT2/+}$; $Rosa26^{LacZ/LacZ}$ (*Wt1*$^{tm2(cre/ERT2)Wtp}$; *Gt(ROSA)26Sor/J*) (Soriano, 1999, Zhou et al., 2008), $Wt1^{CreERT2/co}$; $Rosa26^{LacZ/LacZ}$ (*Wt1*$^{tm2(cre/ERT2)Wtp}$; *Wt1*$^{tm1.1Ndha}$; *Gt(ROSA)26Sor/J*) (Martinez-Estrada et al., 2010), $Wt1^{CreERT2}$; $Rosa26^{mTmG/+}$ (*Wt1*$^{tm2(cre/ERT2)Wtp}$; *Gt(ROSA)26Sor*$^{tm4(ACTB-tdTomato,-EGFP)Luo}$*/J*) (Muzumdar et al., 2007), $Wt1^{CreERT2}$; $Rosa26^{LacZ/mTmG}$ (*Wt1*$^{tm2(cre/ERT2)Wtp}$; *Gt(ROSA)26Sor/J*; *Gt(ROSA)26Sor*$^{tm4(ACTB-tdTomato,-EGFP)Luo}$*/J*) and $Wt1^{CreERT2}$; $Rosa26^{Confetti/+}$ (*Wt1*$^{tm2(cre/ERT2)Wtp}$; *Gt(ROSA)26Sor*$^{tm1(CAG-Brainbow2.1)Cle}$*/J*) (Livet et al., 2007, Snippert et al., 2010). Mice were housed in individually ventilated cages under a 12-hour light/dark cycle, with *ad libitum* access to standard food and water. All animal experiments were performed under a Home Office licence granted under the UK Animals (Scientific Procedures) Act 1986 and were approved by the University of Liverpool ethics committee. Experiments are reported in line with the ARRIVE guidelines.

Tamoxifen dosing

Both male and female animals were used in this study. For lineage tracing in adults, 8- to 10-week-old animals were dosed with 100 μg/g body weight of tamoxifen (T5648, SigmaAldrich; 40 mg/ml, in corn oil (C8267, SigmaAldrich)) via oral gavage on 5 consecutive days. Lineage tracing analysis was undertaken at chase times of 2 weeks, after a 10-day wash-out phase, or 5 ($Wt1^{CreERT2/+}$; $Rosa26^{Confetti/+}$) to 6 ($Wt1^{CreERT2/+}$; $Rosa26^{LacZ/LacZ}$) months. For newborn and embryo lineage tracing experiments, $Wt1^{CreERT2/+}$; $Rosa26^{LacZ/LacZ}$ or $Wt1^{CreERT2/+}$; $Rosa26^{mTmG/mTmG}$ male mice were mated with CD1 females (Charles River, Harlow, UK); when a vaginal plug was detected, noon of the day was considered as embryonic day 0.5 (E0.5). For newborn lineage tracing, tamoxifen (100 μg/g body

weight) was given by oral gavage to the dams at days 1 and 4 after birth, and analysis was performed after a chase of 7 weeks. For embryonic lineage tracing, we administered tamoxifen (100 μg/g body weight) once to pregnant CD1 female mice (Charles River, Harlow, UK) at stages between E14.5 and E7.5, followed by analysis just before birth (E17.5-E19.5).

For ablation of Wt1 in adults, animals were dosed with tamoxifen (100 μg/g body weight) via oral gavage on 5 consecutive days. Animals were monitored for their well-being, and typically culled at day 10 after the start of the tamoxifen regime.

XGal staining and histology

Tissues and embryos were fixed in 2% paraformaldehyde (PFA)/0.25% glutaraldehyde in phosphate buffered saline (PBS) for between 1 and 1.5 hours, whole-mount XGal staining performed overnight according to standard protocols, followed by overnight post-fixation in 4% PFA (PBS) at 4°C. Histological analysis was performed on post-fixed XGal-stained specimen after dehydration into isopropanol and paraffin embedding. Serial sections (7 mm) were counterstained with Eosin and images taken on a Leica DMRB upright microscope with a digital DFC450 C camera supported by LAS.

Immunofluorescence on frozen sections

Embryos or tissues were fixed in 4% PFA for between 30 to 90 mins, protected in 30% sucrose overnight, placed in Cryomatrix (Thermo Scientific) and snap frozen. Frozen sections were generated at 7 mm on a Thermo Scientific HM525 NX Cryostat. Immunofluorescence analysis was performed following standard protocols(Wilm et al., 2005). A bleaching step of 10 min in 3% H_2O_2/MetOH was included for embryos or tissues from $Wt1^{CreERT2}$; $Rosa26^{mTmG/+}$ mice in order to remove the tdTomato fluorescence (Lua et al., 2015). The following primary antibodies were used: anti-Wt1 rabbit polyclonal (1:200 to 1:500, clone C-19, sc-192, Santa Cruz), anti-Wt1 mouse monoclonal (1:50, clone 6F-H2, M3561, Dako), anti-pan-cytokeratin rabbit polyclonal at (1:500 to

1:2000, Z0622, Dako), anti-SMA mouse monoclonal (1:100 to 1:200, clone 1A4, A2547, Sigma), anti-Pecam/CD31 rat monoclonal (1:50, 550274, Pharmingen), anti-GFP rabbit or goat polyclonal (1:5000, ab6556 or ab6673, Abcam). The anti-SMA antibody was directly labeled using Zenon direct labeling kit (Invitrogen/ThermoScientific) according to manufacturer's instructions. Secondary antibodies were Alexa fluorophore-coupled (Invitrogen/ThermoScientific) and were used at a dilution of 1:1000. Sections were counterstained with DAPI (D9542, SigmaAldrich) at 1:1000, coverslipped with Fluoro-Gel (with Tris buffer; Electron Microscopy Sciences, USA), and imaged on a Leica DM 2500 upright microscope with a Leica DFC350 FX digital camera and LAS.

Whole mount in situ hybridization

Mouse embryos from CD1 time matings (Charles River, Harlow, UK) were dissected at between E7.5 and E10.5. The *Wt1* full-length cDNA probe was a gift from the Kreidberg lab (Gao et al., 2005, Pelletier et al., 1991). In situ hybridization was performed following published protocols (Wilm et al., 2004, Hogan et al., 1994). In short, the linearized *Wt1* probe was labeled using the DIG-RNA labelling mix (Roche), and hybridization performed under RNAse-free conditions using 50% Formamide, 5x SSC at 70°C.

Light sheet microscopy

The trunk area of E9.5 $Wt1^{CreERT2/+}$; $Rosa26^{mTmG/+}$ embryos after tamoxifen dosing at E8.5 was dissected out and stored for 1-2 days in PBS at 4˚C in the dark. Samples were prepared by mounting the tissue in 1% low melting point agarose (ROTI Garose, Carl Roth, Karlsruhe, Germany) in PBS in size 4 capillaries (Brand GmbH, Wertheim, Germany). A Zeiss Light sheet Z.1 microscope was used to capture 3D images which were documented on the Zen software (Carl Zeiss, Jena, Germany) by using one 5x detection objective and two 5x illumination objectives. The 488 nm channel was used to detect Wt1-derived GFP+ cells, while the 561 nm channel was used to visualize the membrane-bound dTomato, to support with orientation and tissue context.

Image analysis

Whole mount imaging with and without fluorescence: Imaging of embryos and tissues was performed using a Leica MZ 16F dissecting microscope equipped with a Leica DFC420 C digital camera supported by the Leica Application Suite software package (LAS, version 3 or 4; Leica Microsystems, Germany/Switzerland), and Leica EL6000 fluorescence light source.

Due to uneven tissue geometry, images were taken at different focal levels and subsequently assembled to multilayer composites according to highest focal sharpness.

Confetti imaging: Tissues were imaged in form of multilayer Z-stacks with a 3i spinning disk confocal microscope system (Intelligent Imaging Innovations Ltd.) and images subsequently rendered to Z-projection composites using Fiji ImageJ software. For the short- and long-term chase experiments two groups of three animals each were analysed. The small intestine was dissected, cut into 2-3 cm long segments and sliced flat. Four 2 cm long thin tissue segments were randomly chosen and cleaned from feces by multiple PBS washes. Slides were prepared by gluing two layers of 2x22mm coverslips on a standard slide to form an inner rectangular area for tissue placement to prevent leakage during subsequent inverted confocal microscopy. Tissue samples were placed into the space in the correct orientation, PBS added, covered with a standard 22x40mm coverslip and sealed with clear nail polish. Due to the uneven tissue geometry Z-stack images were taken at random where RFP, YFP and CFP cell labelling was identified in close proximity, in some cases any two of the three possible markers. Cells were scored and counted for all three markers in all Z-stacks according to either being a single cell with or without direct contact to a cell of different marker or being in direct contact with another cell(s) of the same marker (designated clones). Statistical analysis was performed by unpaired multiple t-tests with Holm-Šídák multiple comparisons correction using Graphpad Prism 8.4.2.

3D Image analysis: 3D images and movies were generated by using IMARIS x64 software (version 9.5.1 Bitplane). IMARIS tools used were Rendering, Slices, Orthoslicer, Snapshot images,

Animations, Rotations, Surfaces around the samples, and Spots to show the location of the cells in the movies. The images were cropped and assembled by using Photoshop 2020.

Acknowledgements

We acknowledge funding from the Wellcome Trust project grant WT091374MA (BW, NH, TB, TPW) and the Wellcome Trust PhD programme WT102172 (KW, BM, HT), from the MRC project grant MR/M012751/1 (BW, TPW), from Albaha University, Saudi Arabia (SA), for an institutionally funded PhD (JA), an MBiolSci funded by The NHS Student Bursary (SB), and self-funded MRes (LC, FM, VF). We acknowledge funding by the BBSRC Alert13, grant number BB/L014947/1, for the Zeiss Z.1 Light sheet microscope. We express our thanks to the Biomedical Services Unit and the Centre for Cell Imaging, both at the University of Liverpool, for expert support in mouse maintenance, breeding and time matings, and for expert support in image analysis of the light sheet data, respectively. We acknowledge Sumaya Dauleh for technical assistance.

Author contribution statement

SA, TPW and BW designed the experiments, and SA, TPW, SB, MB, HT, FM, JA, VF, BM, LC, KW, TBe performed experiments. SA, TPW, SB, MB, TBu contributed to data interpretation. TPW and BW designed the figures. NH and BW contributed to the conception and design of the manuscript. BW wrote the manuscript and all authors were responsible for the approval of the manuscript.

References

ARMSTRONG, J. F., PRITCHARD-JONES, K., BICKMORE, W. A., HASTIE, N. D. & BARD, J. B. 1993. The expression of the Wilms' tumour gene, WT1, in the developing mammalian embryo. *Mech Dev,* 40**,** 85-97.

ASAHINA, K., TSAI, S. Y., LI, P., ISHII, M., MAXSON, R. E., JR., SUCOV, H. M. & TSUKAMOTO, H. 2009. Mesenchymal origin of hepatic stellate cells, submesothelial cells,

and perivascular mesenchymal cells during mouse liver development. *Hepatology,* 49**,** 998-1011.

ASAHINA, K., ZHOU, B., PU, W. T. & TSUKAMOTO, H. 2011. Septum transversum-derived mesothelium gives rise to hepatic stellate cells and perivascular mesenchymal cells in developing mouse liver. *Hepatology,* 53**,** 983-95.

BENTZON, J. F. & MAJESKY, M. W. 2018. Lineage tracking of origin and fate of smooth muscle cells in atherosclerosis. *Cardiovasc Res,* 114**,** 492-500.

BOULLAND, J. L., LAMBERT, F. M., ZUCHNER, M., STROM, S. & GLOVER, J. C. 2013. A neonatal mouse spinal cord injury model for assessing post-injury adaptive plasticity and human stem cell integration. *PLoS One,* 8**,** e71701.

BUECHLER, M. B., KIM, K. W., ONUFER, E. J., WILLIAMS, J. W., LITTLE, C. C., DOMINGUEZ, C. X., LI, Q., SANDOVAL, W., COOPER, J. E., HARRIS, C. A., JUNTTILA, M. R., RANDOLPH, G. J. & TURLEY, S. J. 2019. A Stromal Niche Defined by Expression of the Transcription Factor WT1 Mediates Programming and Homeostasis of Cavity-Resident Macrophages. *Immunity,* 51**,** 119-130 e5.

CAO, J. & POSS, K. D. 2018. The epicardium as a hub for heart regeneration. *Nat Rev Cardiol,* 15**,** 631-647.

CARMONA, R., CANO, E., MATTIOTTI, A., GAZTAMBIDE, J. & MUNOZ-CHAPULI, R. 2013. Cells derived from the coelomic epithelium contribute to multiple gastrointestinal tissues in mouse embryos. *PLoS One,* 8**,** e55890.

CHAU, Y. Y., BANDIERA, R., SERRELS, A., MARTINEZ-ESTRADA, O. M., QING, W., LEE, M., SLIGHT, J., THORNBURN, A., BERRY, R., MCHAFFIE, S., STIMSON, R. H., WALKER, B. R., CHAPULI, R. M., SCHEDL, A. & HASTIE, N. 2014. Visceral and subcutaneous fat have different origins and evidence supports a mesothelial source. *Nat Cell Biol,* 16**,** 367-75.

CHAU, Y. Y., BROWNSTEIN, D., MJOSENG, H., LEE, W. C., BUZA-VIDAS, N., NERLOV, C., JACOBSEN, S. E., PERRY, P., BERRY, R., THORNBURN, A., SEXTON, D., MORTON, N., HOHENSTEIN, P., FREYER, E., SAMUEL, K., VAN'T HOF, R. & HASTIE, N. 2011. Acute multiple organ failure in adult mice deleted for the developmental regulator Wt1. *PLoS Genet,* 7**,** e1002404.

CHEN, Y. T., CHANG, Y. T., PAN, S. Y., CHOU, Y. H., CHANG, F. C., YEH, P. Y., LIU, Y. H., CHIANG, W. C., CHEN, Y. M., WU, K. D., TSAI, T. J., DUFFIELD, J. S. & LIN, S. L. 2014. Lineage tracing reveals distinctive fates for mesothelial cells and submesothelial fibroblasts during peritoneal injury. *J Am Soc Nephrol,* 25**,** 2847-58.

COLUNGA, T., HAYWORTH, M., KRESS, S., REYNOLDS, D. M., CHEN, L., NAZOR, K. L., BAUR, J., SINGH, A. M., LORING, J. F., METZGER, M. & DALTON, S. 2019. Human Pluripotent Stem Cell-Derived Multipotent Vascular Progenitors of the Mesothelium Lineage Have Utility in Tissue Engineering and Repair. *Cell Rep,* 26**,** 2566-2579 e10.

DAULEH, S., SANTERAMO, I., FIELDING, C., WARD, K., HERRMANN, A., MURRAY, P. & WILM, B. 2016. Characterisation of cultured mesothelial cells derived from the murine adult omentum. *PLoS ONE,* 11.

GAO, X., CHEN, X., TAGLIENTI, M., RUMBALLE, B., LITTLE, M. H. & KREIDBERG, J. A. 2005. Angioblast-mesenchyme induction of early kidney development is mediated by Wt1 and Vegfa. *Development,* 132**,** 5437-49.

HAQUE, F., RANCIC, V., ZHANG, W., CLUGSTON, R., BALLANYI, K. & GOSGNACH, S. 2018. WT1-Expressing Interneurons Regulate Left-Right Alternation during Mammalian Locomotor Activity. *J Neurosci,* 38**,** 5666-5676.

HARTMAN, H. A., LAI, H. L. & PATTERSON, L. T. 2007. Cessation of renal morphogenesis in mice. *Dev Biol,* 310**,** 379-87.

HOGAN, B. L. M., BEDDINGTON, R., COSTANTINI, F. & LACY, E. 1994. *Manipulating the Mouse Embryo: A Laboratory Manual*, Cold Spring Harbor Laboratory Press.

KARKI, S., SUROLIA, R., HOCK, T. D., GUROJI, P., ZOLAK, J. S., DUGGAL, R., YE, T., THANNICKAL, V. J. & ANTONY, V. B. 2014. Wilms' tumor 1 (Wt1) regulates pleural mesothelial cell plasticity and transition into myofibroblasts in idiopathic pulmonary fibrosis. *FASEB J,* 28**,** 1122-31.

KENDALL, T. J., DUFF, C. M., BOULTER, L., WILSON, D. H., FREYER, E., AITKEN, S., FORBES, S. J., IREDALE, J. P. & HASTIE, N. D. 2019. Embryonic mesothelial-derived hepatic lineage of quiescent and heterogenous scar-orchestrating cells defined but suppressed by WT1. *Nat Commun,* 10**,** 4688.

KUMAR, A., D'SOUZA, S. S., MOSKVIN, O. V., TOH, H., WANG, B., ZHANG, J., SWANSON, S., GUO, L. W., THOMSON, J. A. & SLUKVIN, II 2017. Specification and Diversification of Pericytes and Smooth Muscle Cells from Mesenchymoangioblasts. *Cell Rep,* 19**,** 1902-1916.

LI, Y., WANG, J. & ASAHINA, K. 2013. Mesothelial cells give rise to hepatic stellate cells and myofibroblasts via mesothelial-mesenchymal transition in liver injury. *Proc Natl Acad Sci U S A,* 110**,** 2324-9.

LIVET, J., WEISSMAN, T. A., KANG, H., DRAFT, R. W., LU, J., BENNIS, R. A., SANES, J. R. & LICHTMAN, J. W. 2007. Transgenic strategies for combinatorial expression of fluorescent proteins in the nervous system. *Nature,* 450**,** 56-62.

LUA, I., LI, Y., PAPPOE, L. S. & ASAHINA, K. 2015. Myofibroblastic Conversion and Regeneration of Mesothelial Cells in Peritoneal and Liver Fibrosis. *Am J Pathol,* 185**,** 3258-73.

MAJESKY, M. W. 2018. Vascular Development. *Arterioscler Thromb Vasc Biol,* 38**,** e17-e24.

MARTINEZ-ESTRADA, O. M., LETTICE, L. A., ESSAFI, A., GUADIX, J. A., SLIGHT, J., VELECELA, V., HALL, E., REICHMANN, J., DEVENNEY, P. S., HOHENSTEIN, P., HOSEN, N., HILL, R. E., MUNOZ-CHAPULI, R. & HASTIE, N. D. 2010. Wt1 is required for cardiovascular progenitor cell formation through transcriptional control of Snail and E-cadherin. *Nat Genet,* 42**,** 89-93.

MOORE, A. W., SCHEDL, A., MCINNES, L., DOYLE, M., HECKSHER-SORENSEN, J. & HASTIE, N. D. 1998. YAC transgenic analysis reveals Wilms' tumour 1 gene activity in the proliferating coelomic epithelium, developing diaphragm and limb. *Mech Dev,* 79**,** 169-84.

MUTSAERS, S. E. 2004. The mesothelial cell. *Int J Biochem Cell Biol,* 36**,** 9-16.

MUTSAERS, S. E., BIRNIE, K., LANSLEY, S., HERRICK, S. E., LIM, C. B. & PRELE, C. M. 2015. Mesothelial cells in tissue repair and fibrosis. *Front Pharmacol,* 6**,** 113.

MUZUMDAR, M. D., TASIC, B., MIYAMICHI, K., LI, L. & LUO, L. 2007. A global double-fluorescent Cre reporter mouse. *Genesis,* 45**,** 593-605.

NAKAMURA, E., NGUYEN, M. T. & MACKEM, S. 2006. Kinetics of tamoxifen-regulated Cre activity in mice using a cartilage-specific CreER(T) to assay temporal activity windows along the proximodistal limb skeleton. *Dev Dyn,* 235**,** 2603-12.

NAMVAR, S., WOOLF, A. S., ZEEF, L. A., WILM, T., WILM, B. & HERRICK, S. E. 2018. Functional molecules in mesothelial-to-mesenchymal transition revealed by transcriptome analyses. *J Pathol,* 245**,** 491-501.

PELLETIER, J., SCHALLING, M., BUCKLER, A. J., ROGERS, A., HABER, D. A. & HOUSMAN, D. 1991. Expression of the Wilms' tumor gene WT1 in the murine urogenital system. *Genes Dev,* 5**,** 1345-56.

PORRELLO, E. R., MAHMOUD, A. I., SIMPSON, E., HILL, J. A., RICHARDSON, J. A., OLSON, E. N. & SADEK, H. A. 2011. Transient regenerative potential of the neonatal mouse heart. *Science,* 331**,** 1078-80.

PORRELLO, E. R. & OLSON, E. N. 2014. A neonatal blueprint for cardiac regeneration. *Stem Cell Res,* 13**,** 556-70.

QUE, J., WILM, B., HASEGAWA, H., WANG, F., BADER, D. & HOGAN, B. L. 2008. Mesothelium contributes to vascular smooth muscle and mesenchyme during lung development. *Proc Natl Acad Sci U S A,* 105**,** 16626-30.

QUIJADA, P., TREMBLEY, M. A. & SMALL, E. M. 2020. The Role of the Epicardium During Heart Development and Repair. *Circ Res,* 126**,** 377-394.

RED-HORSE, K., UENO, H., WEISSMAN, I. L. & KRASNOW, M. A. 2010. Coronary arteries form by developmental reprogramming of venous cells. *Nature,* 464**,** 549-53.

ROOSTALU, U. & WONG, J. K. 2018. Arterial smooth muscle dynamics in development and repair. *Dev Biol,* 435**,** 109-121.

RUDAT, C. & KISPERT, A. 2012. Wt1 and epicardial fate mapping. *Circ Res,* 111**,** 165-9.

SAGA, Y., HATA, N., KOBAYASHI, S., MAGNUSON, T., SELDIN, M. F. & TAKETO, M. M. 1996. MesP1: a novel basic helix-loop-helix protein expressed in the nascent mesodermal cells during mouse gastrulation. *Development,* 122**,** 2769-78.

SEELY, J. C. 2017. A brief review of kidney development, maturation, developmental abnormalities, and drug toxicity: juvenile animal relevancy. *J Toxicol Pathol,* 30**,** 125-133.

SERETI, K. I., NGUYEN, N. B., KAMRAN, P., ZHAO, P., RANJBARVAZIRI, S., PARK, S., SABRI, S., ENGEL, J. L., SUNG, K., KULKARNI, R. P., DING, Y., HSIAI, T. K., PLATH, K., ERNST, J., SAHOO, D., MIKKOLA, H. K. A., IRUELA-ARISPE, M. L. & ARDEHALI, R. 2018. Analysis of cardiomyocyte clonal expansion during mouse heart development and injury. *Nat Commun,* 9**,** 754.

SMART, N., BOLLINI, S., DUBE, K. N., VIEIRA, J. M., ZHOU, B., DAVIDSON, S., YELLON, D., RIEGLER, J., PRICE, A. N., LYTHGOE, M. F., PU, W. T. & RILEY, P. R. 2011. De novo cardiomyocytes from within the activated adult heart after injury. *Nature,* 474**,** 640-4.

SNIPPERT, H. J., VAN DER FLIER, L. G., SATO, T., VAN ES, J. H., VAN DEN BORN, M., KROON-VEENBOER, C., BARKER, N., KLEIN, A. M., VAN RHEENEN, J., SIMONS, B. D. & CLEVERS, H. 2010. Intestinal crypt homeostasis results from neutral competition between symmetrically dividing Lgr5 stem cells. *Cell,* 143**,** 134-44.

SORIANO, P. 1999. Generalized lacZ expression with the ROSA26 Cre reporter strain. *Nat Genet,* 21**,** 70-1.

TIAN, X., HU, T., ZHANG, H., HE, L., HUANG, X., LIU, Q., YU, W., HE, L., YANG, Z., ZHANG, Z., ZHONG, T. P., YANG, X., YANG, Z., YAN, Y., BALDINI, A., SUN, Y., LU, J., SCHWARTZ, R. J., EVANS, S. M., GITTENBERGER-DE GROOT, A. C., RED-HORSE, K. & ZHOU, B. 2013. Subepicardial endothelial cells invade the embryonic ventricle wall to form coronary arteries. *Cell Res,* 23**,** 1075-90.

VON GISE, A., STEVENS, S. M., HONOR, L. B., OH, J. H., GAO, C., ZHOU, B. & PU, W. T. 2016. Contribution of Fetal, but Not Adult, Pulmonary Mesothelium to Mesenchymal Lineages in Lung Homeostasis and Fibrosis. *Am J Respir Cell Mol Biol,* 54**,** 222-30.

WANG, G., JACQUET, L., KARAMARITI, E. & XU, Q. 2015. Origin and differentiation of vascular smooth muscle cells. *J Physiol,* 593**,** 3013-30.

WILM, B., IPENBERG, A., HASTIE, N. D., BURCH, J. B. E. & BADER, D. M. 2005. The serosal mesothelium is a major source of smooth muscle cells of the gut vasculature. *Development,* 132**,** 5317-5328.

WILM, B., JAMES, R. G., SCHULTHEISS, T. M. & HOGAN, B. L. 2004. The forkhead genes, Foxc1 and Foxc2, regulate paraxial versus intermediate mesoderm cell fate. *Dev Biol,* 271**,** 176-89.

WILM, B. & MUNOZ-CHAPULI, R. 2016. Tools and Techniques for Wt1-Based Lineage Tracing. *Methods Mol Biol,* 1467**,** 41-59.

WINTERS, N. I., THOMASON, R. T. & BADER, D. M. 2012. Identification of a novel developmental mechanism in the generation of mesothelia. *Development,* 139**,** 2926-34.

ZHOU, B., HONOR, L. B., HE, H., MA, Q., OH, J. H., BUTTERFIELD, C., LIN, R. Z., MELERO-MARTIN, J. M., DOLMATOVA, E., DUFFY, H. S., GISE, A., ZHOU, P., HU, Y. W., WANG, G., ZHANG, B., WANG, L., HALL, J. L., MOSES, M. A., MCGOWAN, F. X. & PU, W. T. 2011. Adult mouse epicardium modulates myocardial injury by secreting paracrine factors. *J Clin Invest,* 121**,** 1894-904.

ZHOU, B., MA, Q., RAJAGOPAL, S., WU, S. M., DOMIAN, I., RIVERA-FELICIANO, J., JIANG, D., VON GISE, A., IKEDA, S., CHIEN, K. R. & PU, W. T. 2008. Epicardial progenitors contribute to the cardiomyocyte lineage in the developing heart. *Nature,* 454**,** 109-13.

Figures and Figure Legends

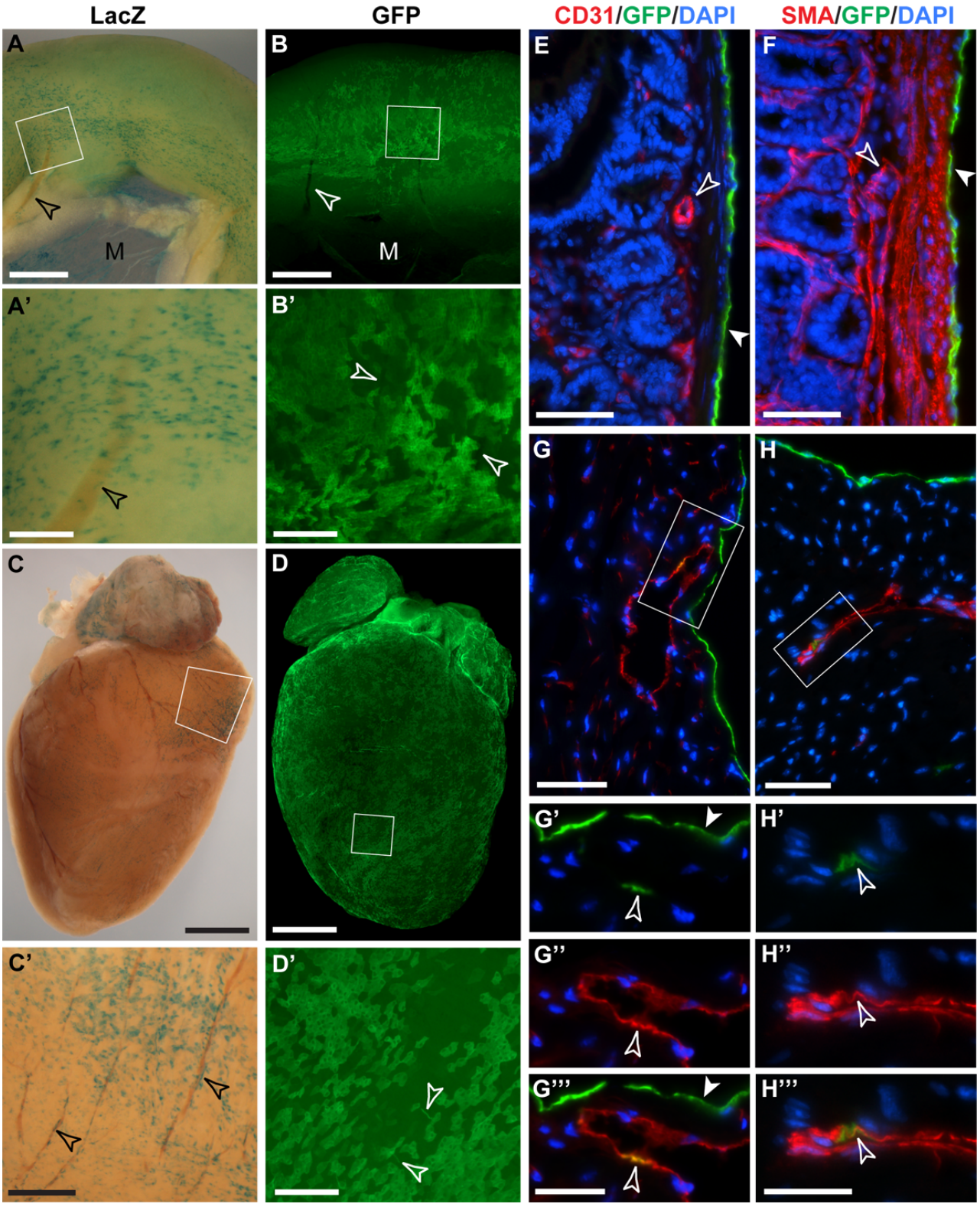

Figure 1: Whole mount and frozen section analysis of adult intestine and heart after lineage tracing of Wt1-expressing cells. Adult mice with either the Wt1^{CreERT2}; Rosa26$^{LacZ/LacZ}$ (A, C) or the Wt1^{CreERT2}; Rosa26$^{mTmG/mTmG}$ (B, D) reporter system were analysed 2-4 weeks after tamoxifen

administration. A, B. labelled cells were found on the surface of the intestine and in the mesentery (M) in a random and patchy distribution but no contribution of labelled cells to the vascular or visceral smooth muscle of the intestine or mesentery was observed (open arrowheads; A', B', magnifications of highlighted areas). C, D. Similarly to the intestine, coverage of the epicardium with labelled cells was patchy. C', D'. Magnification of highlighted areas in C and D. LacZ-positive cells appeared to localize around coronary vessels (arrowheads) in addition to presence in the epicardium. By contrast, GFP-labelled cells consisted predominantly of flat-shaped epicardial cells, with a few thinly shaped cells detectable (open arrowheads). E-H. Immunofluorescence labelling of frozen sections from $Wt1^{CreERT2}$; $Rosa26^{mTmG/mTmG}$ intestine and heart tissue. E, F. In the intestine, Wt1-lineage traced cells were solely identified in the mesothelium (filled arrowheads; open arrowheads pointing to vascular tissue labelled with endothelial CD31 and α-smooth muscle actin (SMA) antibodies). G, H. In the heart, co-expression of GFP with CD31 or SMA, respectively, was observed in coronary vasculature. G'-G''', H'-H'''. Magnification of areas highlighted in G and H. GFP and DAPI (G', H'); CD31 or SMA and DAPI (G'', H''), merged (G''',H'''; co-localization highlighted by arrow heads). Scale bars, 1 mm (A, B), 200 μm (A', B'), 1.5 mm (C, D), 400 μm (C'), 200 μm (D'), 50 μm (E-H), 25 μm (G'-G''', H'-H''').

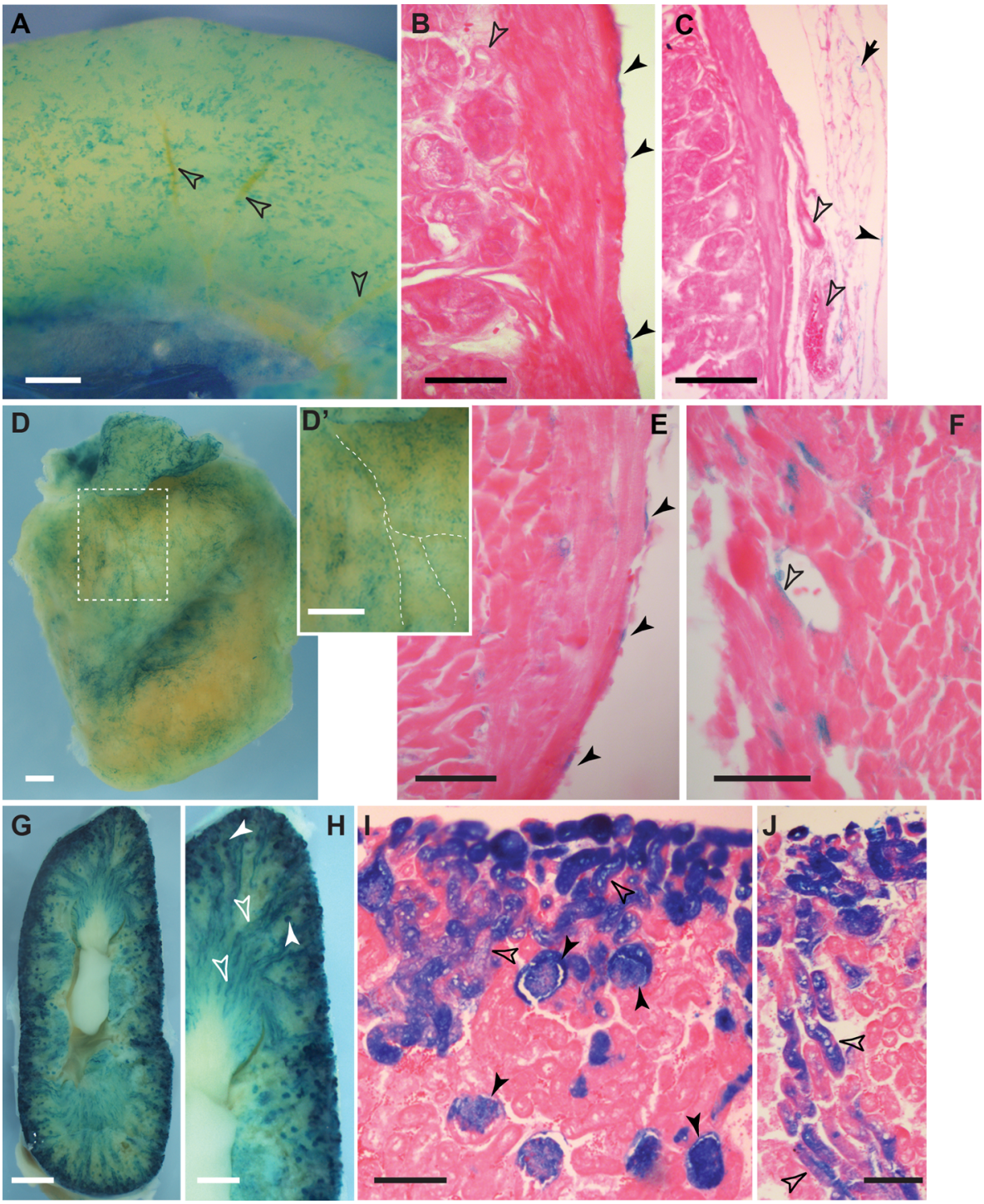

Figure 2. Wt1 lineage tracing in newborn mice. Tamoxifen was given to dams on days 1 and 4 after giving birth. Intestine (A-C), heart (D-F) and kidneys (G-J) of 7 old $Wt1^{CreERT2/+}$;$Rosa26^{LacZ/+}$ were stained by XGal and analysed for labelled cells. In the intestine, only mesothelial cells were labelled (A, B, filled arrowheads), while there were no labelled cells found around blood vessels (open arrowheads, A-C). In the mesentery, mesothelial (filled arrowhead) and fat cells (arrow) also showed XGal staining (C). The heart (left ventricle and atrium shown, D) was covered with XGal

labelled cells localised close to coronary vessels (stippled lines in inset D'). Sections revealed XGal labelling of epicardial cells (filled arrowheads, E), but also of some coronary vessel cells (open arrowhead, F). Labelled cells in the kidneys were abundant throughout (G), predominantly in the glomeruli (H, I, filled arrowheads), but also in nephric tubules (H-J, open arrowheads). Scale bars, 500 μm (A, D, D', H), 1 mm (G), 50 μm (B, E, F), 100 μm (C, I, J).

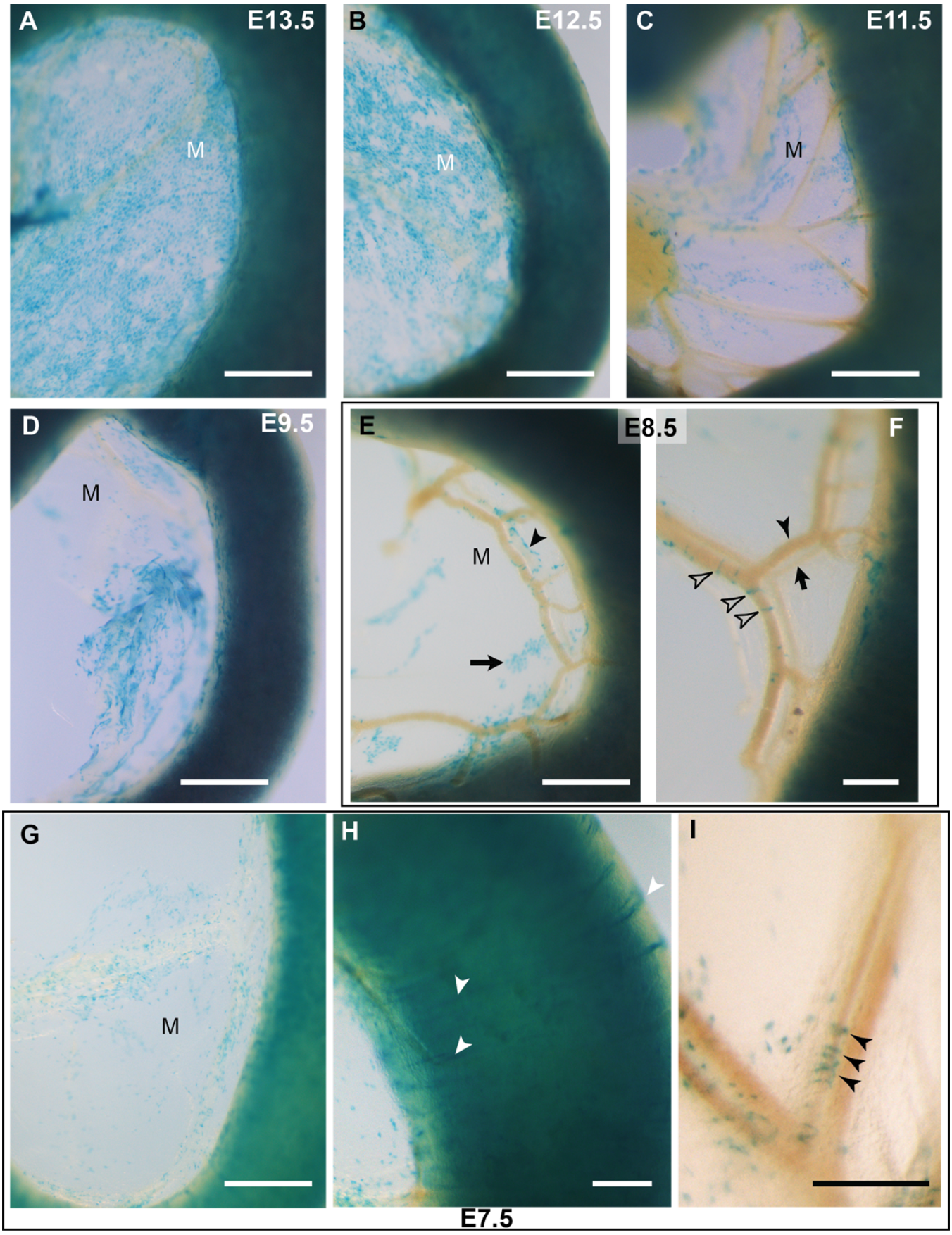

Figure 3. Wt1 lineage tracing in embryos. Tamoxifen was given at the respective embryonic stages to CD1 dams time mated with $Wt1^{CreERT2/+}$;$Rosa26^{LacZ/LacZ}$, embryos dissected between E17.5

and E19.5, and XGal stained. A. When tamoxifen was given at E13.5 and analysed at E17.5, the mesentery (M) and intestine were well covered by lacZ+ cells. B. When tamoxifen had been given at E12.5, the coverage of LacZ-positive cells in the mesentery was less complete at E19.5. This loss of coverage with LacZ-positive cells was still more pronounced E17.5 when tamoxifen had been given at E11.5 (C). D. Similarly, there were only patches of LacZ-positive cells in the mesentery and over the intestine at E17.5 after tamoxifen at E9.5. E, F. When tamoxifen had been given at E8.5, LacZ-positive cells were observed in small patches in the mesentery (arrow, E), or in cell chains near the vasculature (arrowhead, E), or in distinct rings (open arrowheads, F) surrounding the mesenteric veins (filled arrowhead, F) in the second arcade of the mesenteric vascular tree. The corresponding artery is depicted with an arrow (F). G-I. Tamoxifen dosing at E7.5 resulted at E18.5 in LacZ-positive cells scattered within the mesentery (G), in the circular musculature of the small intestine (white arrowheads, H), and surrounding a segment of mesenteric artery of the second arcade (black arrowheads, I). Scale bars, 500 μm (A, B, C, D, E, G), 200 μm (F, H, I).

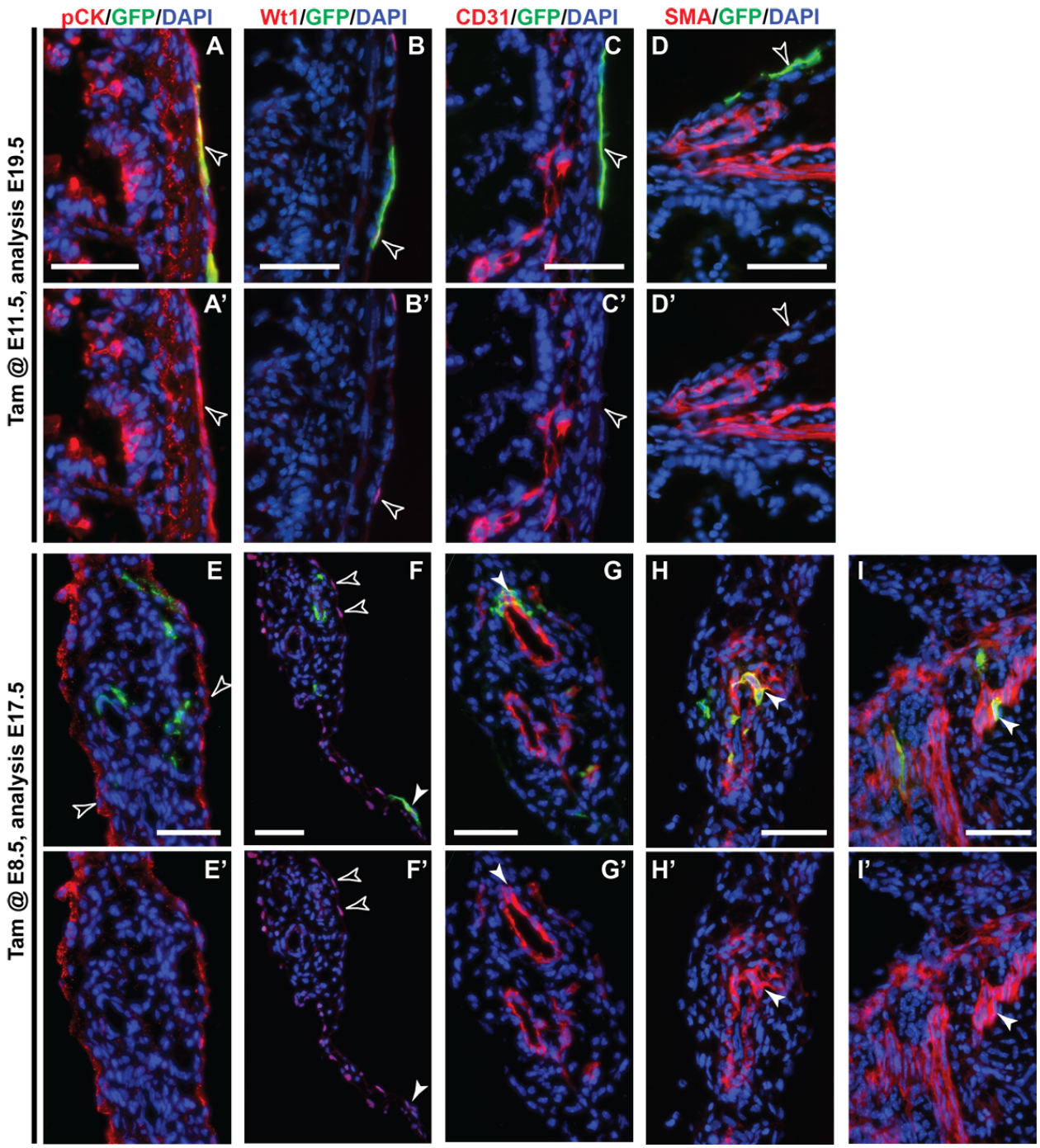

Figure 4. Immunofluorescence analysis of Wt1 lineage in embryos. Frozen sections of intestine and mesentery of embryos (Tamoxifen dosing at E11.5 or E8.5, and dissection at E19.5 or E17.5, respectively) were analysed by immunofluorescence for co-expression of GFP with cytokeratin (A, A', E, E'), Wt1 (B, B', F, F'), CD31 (C, C', G, G') and SMA (D, D' H, H', I, I'). A, A', B, B'. After tamoxifen at E11.5, the mesothelial markers cytokeratin and Wt1 were detected in the mesothelium covering the intestine or mesentery and co-expression with GFP was observed in the visceral mesothelium (arrowheads). E, E', F, F'. After tamoxifen at E8.5, co-expression of GFP

with mesothelial markers was sparse (filled arrowhead). C, C', D, D'. After tamoxifen at E11.5, expression analysis for the vascular markers CD31 and SMA showed no co-expression with GFP. G, G'. After tamoxifen at E8.5, GFP-positive cells were found in close vicinity to CD31 expressed in the mesenteric vessels (arrowhead). H, H', I, I'. At this stage, GFP was co-expressed with SMA in the mesenteric vasculature (arrowhead, H, H'), and the visceral smooth muscle (arrowhead, I, I'). Scale bars, 50 μm (all).

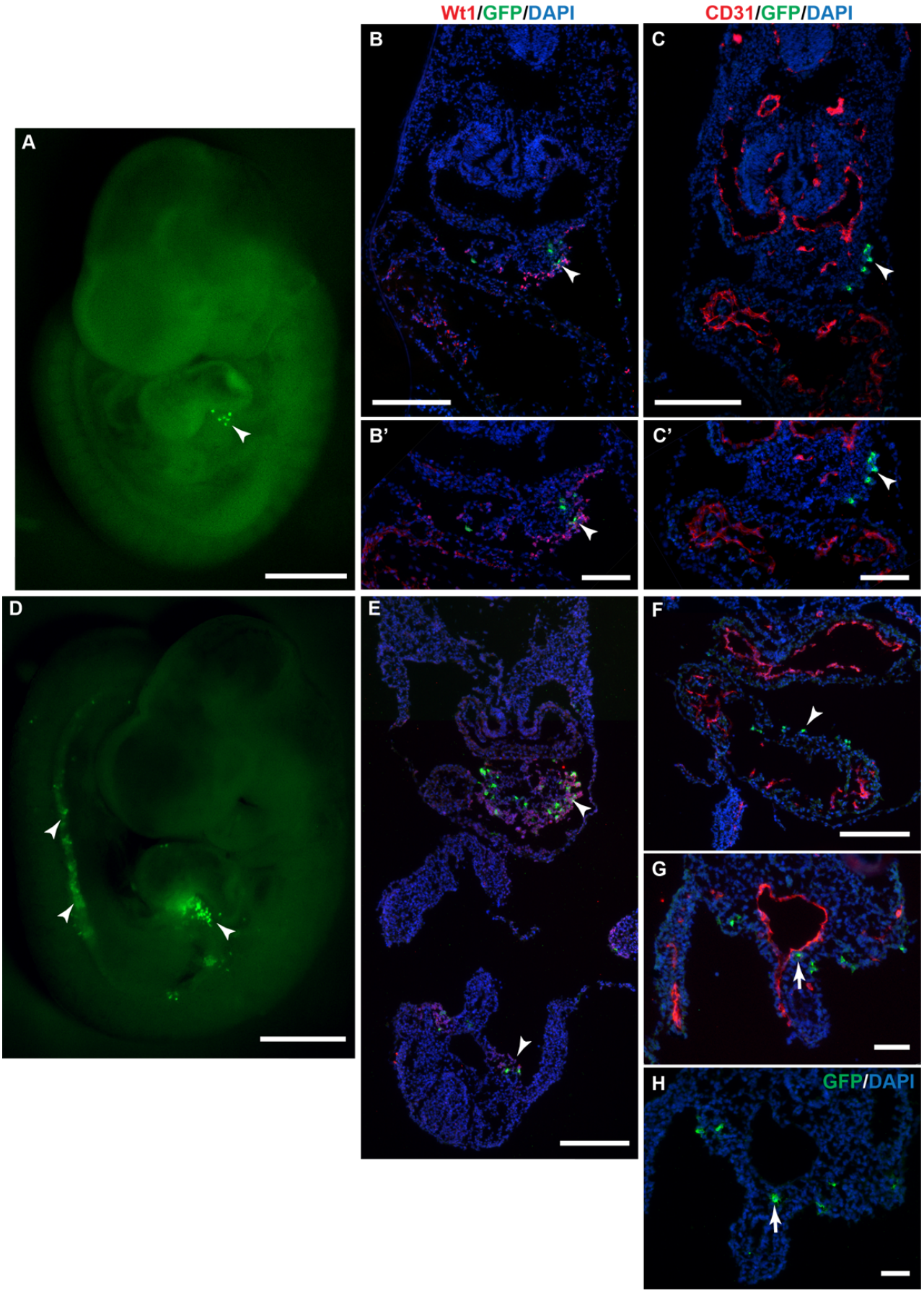

Figure 5. Wt1 lineage analysis at E9.5 after tamoxifen dosing at E7.5 and E8.5. A. Tamoxifen dosing at E7.5 and analysis at E9.5 revealed only a small number of GFP-positive cells in the pro-epicardium (arrowhead). B, B', C, C'. Immunofluorescence analysis of sections of these embryos with GFP and either Wt1 or CD31 confirmed the limited expression in pro-epicardial cells (arrowheads). D. When tamoxifen was administered at E8.5 and followed by analysis at E9.5, GFP-positive cells were detectable in the pro-epicardium and the urogenital ridge (arrowheads). E, F. Immunofluorescence analysis with Wt1 and CD31 on sections of these embryos confirmed this distribution (arrowheads). G, H. In addition, GFP-expressing cells were identified in the mesentery (arrows). Scale bars, 500 μm (A, D), 200 μm (B, C, E, F), 100 μm (B', C'), 50 μm (G, H).

The movies can be downloaded from the following link:

https://doi.org/10.6084/m9.figshare.12834623.v1

Movie 1. 3D viewing animation generated from z-stacks captured with light sheet microscopy shows the location of the GFP-positive cells in the trunk area of an E9.5 embryo after tamoxifen dosing at E8.5. The movie was edited using the IMARIS software to highlight the shape of the selected area by using the surface tool, and by labelling GFP-positive cells with coloured spots to indicate their different locations (white spots: cells in the mesentery, yellow spots: cells in the neural tube, blue spots: cells in the epicardium, green spots: cells in the lateral plate mesoderm. The membrane-bound dTomato appears in red (561 nm) to illustrate the body structure.

Movie 2. The movie illustrates the presence of GFP-positive cells in the mesentery, using views from X-, Y- and Z-axes of a 3D z-stack generated by light sheet microscopy. The animation was generated in IMARIS by using the Ortho slicer tool for each axis.

Supplementary Information

Wt1-expressing cells contribute to mesoderm-derived tissues in intestine and mesentery in two distinct phases during murine embryonic development.

Suad Alghamdi[$1], Thomas P Wilm[$1], Shanthi Beglinger[1], Michael Boyes[1], Helen Tanton[1,3], Fiona Mutter[1], Joanna Allardyce[1,4], Veronica Foisor[1,5], Ben Middlehurst[1], Lauren Carr[1], Kelly Ward[1], Tarek Benameur[1,6], Thomas Butts[1], Nicholas Hastie[2], Bettina Wilm[1^]

[$] contributed equally

Correspondence to: b.wilm@liverpool.ac.uk

List of Supplementary Information:

Supplementary Figures S1 – S12

Supplementary Table 1

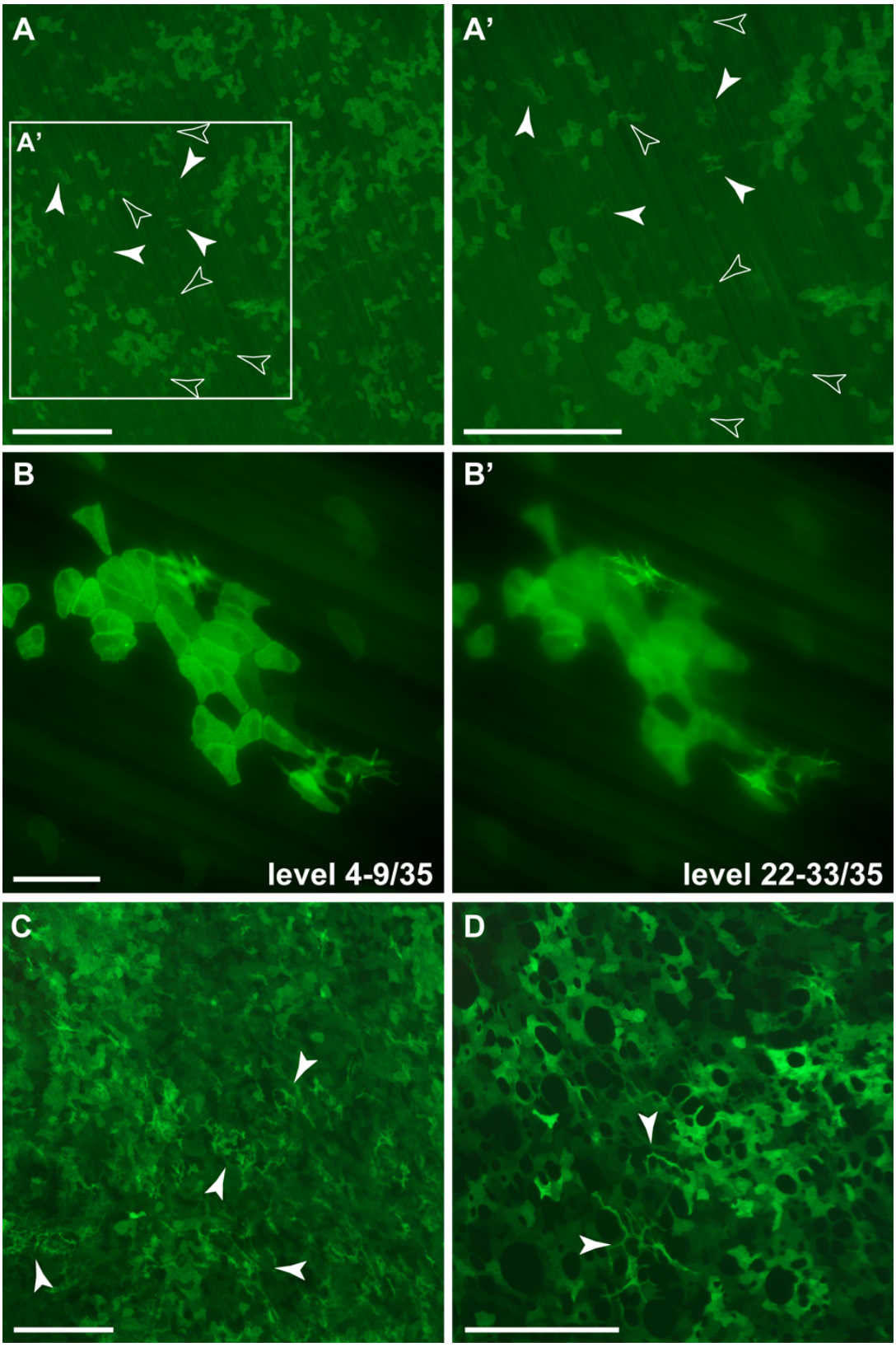

Supplementary Figure S1: Lineage tracing of Wt1-expression GFP-positive mesenchymal cells in parietal and visceral peritoneum. Adult mice with the $Wt1^{CreERT2/+}$; $Rosa26^{mTmG/mTmG}$ reporter system were analysed 2-4 weeks after tamoxifen administration. A, A'. In the parietal peritoneum of the body wall, GFP-positive mesothelial cells were detected in single and clustered

patterns. GFP-positive mesenchymal cells were found in areas without GFP-positive mesothelial cells (solid arrow heads) as well as close to or underneath GFP-positive mesothelial clusters (transparent arrow heads). B, B'. Partial projections of a 0.5 μm distanced 35 focal level Z-stack; levels 4-9 (B) show a cluster of GFP-positive mesothelial cells and levels 22-33 (B') three GFP-positive individual mesenchymal cells located underneath the mesothelial layer. C. GFP-positive mesenchymal cells in the visceral peritoneum of the mesentery. D. GFP-positive mesenchymal cells in the visceral peritoneum of the omentum. Scale bars, 500 μm (A, A', C, D), 200 μm (B, B').

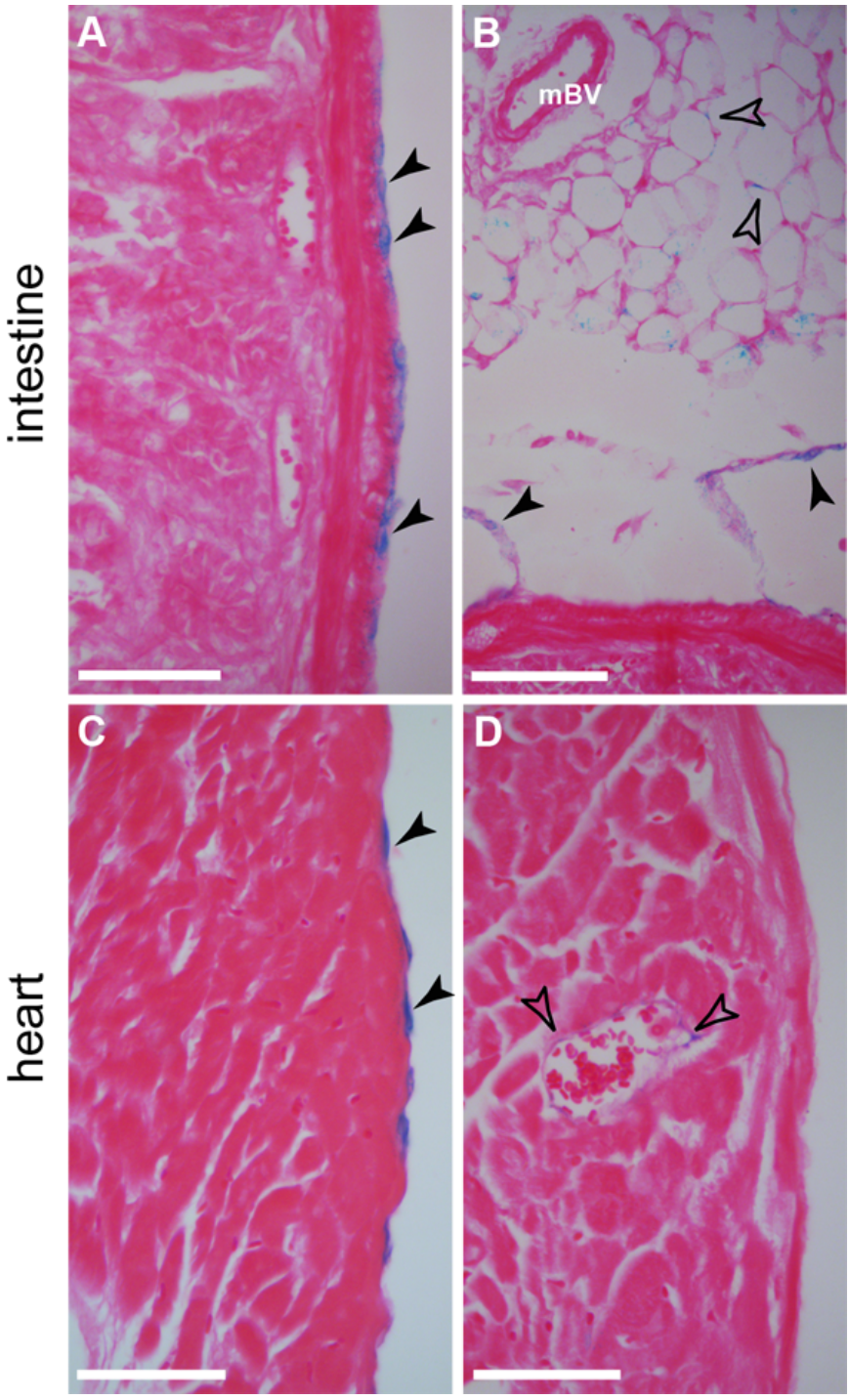

Supplement Figure S2: Histological analysis of mesothelial contribution to adult intestine and heart after lineage tracing of Wt1-expressing cells. Adult $Wt1^{CreERT2/+}$; $Rosa26^{LacZ/LacZ}$ mice were analysed 2-4 weeks after tamoxifen administration. A, B. LacZ-positive cells in eosin counterstained paraffin sections of intestine (A) and mesentery (B) were detected in the serosal mesothelium (solid arrowheads) as well as in the mesenteric fat (open arrowheads); mBV, mesenteric blood vessel. Open arrowhead points towards mesenteric blood vessel. C, D. Eosin

counterstained sections through ventricular wall of the heart revealed LacZ-positive cells in the epicardium (arrowheads, C) and in the coronary vessels (open arrowheads, F). Scale bars, 50 μm (A, C, D), 100 μm (B).

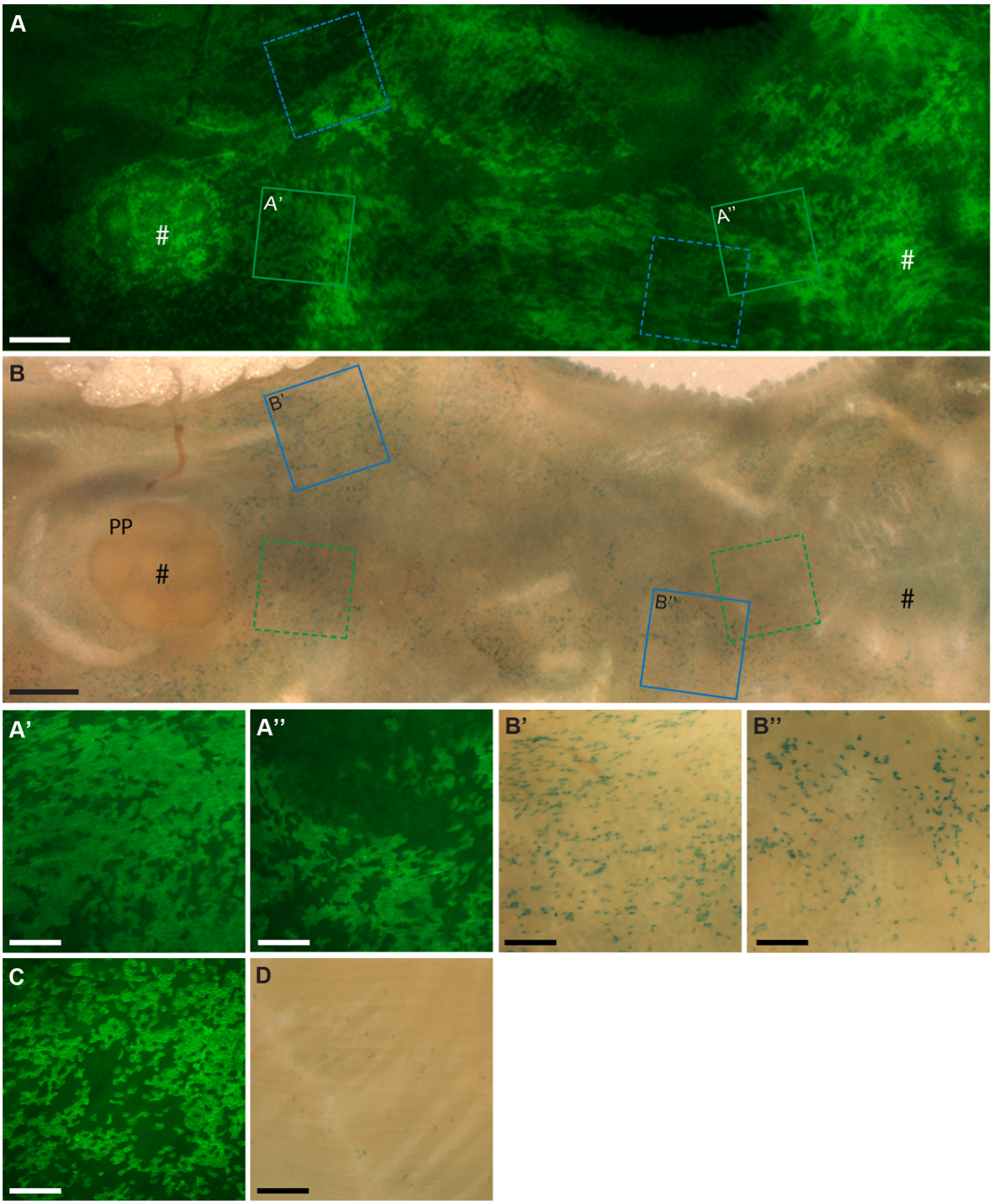

Supplementary Figure S3: Comparison of the distribution of peritoneal GFP- and LacZ-expressing cells in the intestine and body wall muscle after lineage tracing in Wt1$^{CreERT2/+}$; Rosa26$^{LacZ/mTmG}$ reporter mice. A, B. A segment of small intestine was dissected and carefully stretched out on a wax plate using fine insect pins and the profile of the GFP-expressing cells captured (A). The stretched-out tissue segment was then fixed, removed from the wax plate, XGal-stained and reattached to the same wax plate (using matching pin wholes) for capturing of the profile of LacZ-positive cells (B). In direct comparison many more GFP-positive cells overall were

detected than LacZ-positive cells. Also, LacZ-free areas showed much more frequently GFP-positive cells (#) than vice versa. Specific regions of the intestinal tissue were imaged at higher magnification to demonstrate irregular coverage of GFP-expressing (A', A'') or LacZ-expressing cells (B', B''; highlighted in A and B, respectively). C, D. Coverage of GFP-positive cells in the parietal peritoneum (of the body wall muscle layer; same animal) was similarly dense while sparse for LacZ-positive cells. Peyer's patch (PP); scale bars, 1mm (A, B), 300 μm (A', A'', B', B'', C, D).

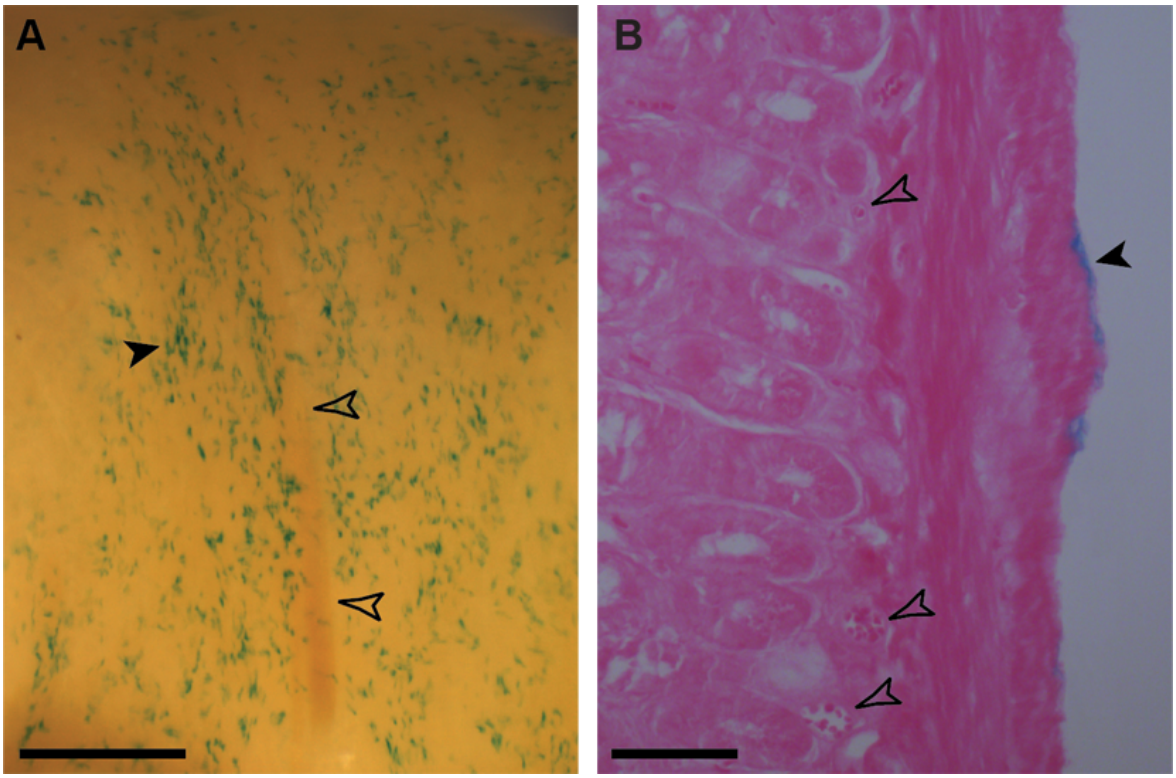

Supplementary Figure S4: Long-term lineage tracing of Wt1-expressing cells in adult mouse intestine. Adult $Wt1^{CreERT2/+}$; $Rosa26^{LacZ/LacZ}$ mice were analysed 2 and 6 months after tamoxifen administration (n = 6 in both groups). A. Whole mount analysis revealed no difference in distribution pattern and patchiness of LacZ expressing cells in the serosal mesothelium in either group (long chase shown only; filled arrowhead pointing to group of neighbouring cells, open arrowheads to blood vessel). B. Eosin counterstained paraffin sections of the same intestinal segment as shown in A, demonstrated LacZ expressing cells in the mesothelium overlying the muscularis of the intestinal wall (filled arrowhead), but no other tissues including the vasculature (open arrowheads). Scale bars, 400 μm (A) and 50 μm (B).

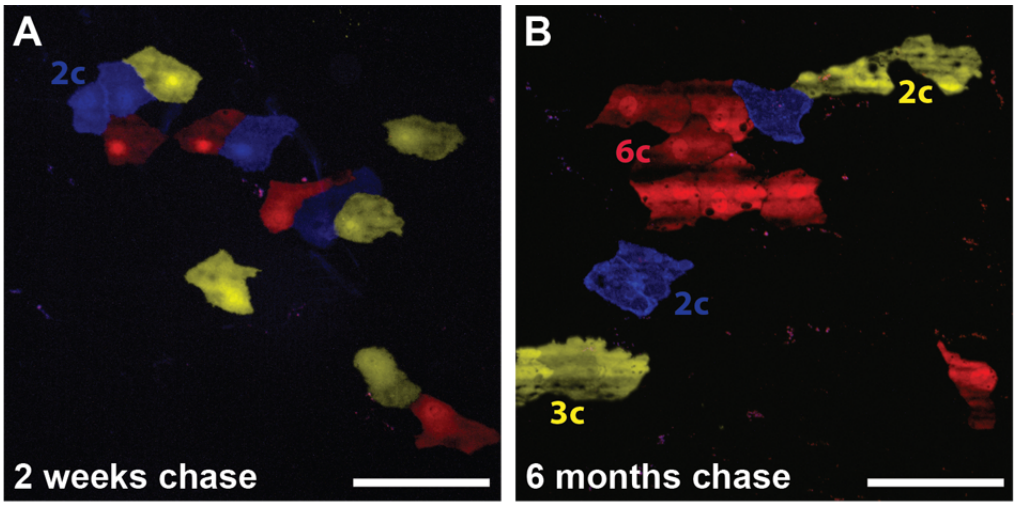

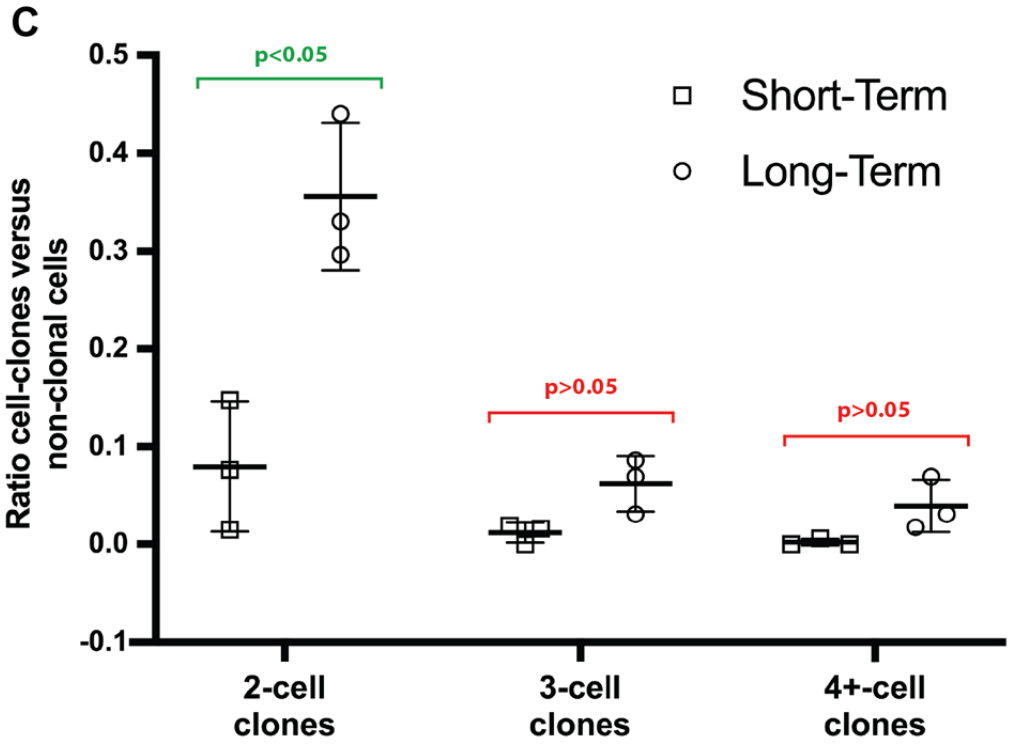

D

	Animal ID	Ratio (x-cell/1-cell)	scans analysed	single cells	cell clones							
					2-cell	3-cell	4-cell	5-cell	6-cell	7-cell	8-cell	(4+-cell)
Short Term Chase	#1		5	68	1	0	0	0	0	0	0	0
	#2		42	677	100	13	2	2	0	0	0	4
	#3		25	430	33	7	0	0	0	0	0	0
	Total		72	1175	134	20	2	2	0	0	0	4
		#1	—	1	0.0147	0.0000						0.0000
		#2	—	1	0.1477	0.0192						0.0059
		#3	—	1	0.0767	0.0163						0.0000
		Total	—	1	0.1140	0.0170	0.0017	0.0017	0.0	0.0	0.0	0.0034
Long Term Chase	#4		57	302	133	26	13	1	7	0	0	21
	#5		112	1119	370	78	26	5	1	2	1	35
	#6		112	516	153	16	7	2	0	0	0	9
	Total		281	1937	656	120	46	8	8	2	1	65
		#4	—	1	0.4404	0.0861						0.0695
		#5	—	1	0.3306	0.0697						0.0313
		#6	—	1	0.2965	0.0310						0.0174
		Total	—	1	0.3387	0.0619	0.024	0.004	0.004	0.001	0.0005	0.0336

Supplementary Figure S5: Clonal analysis of short-term and long-term lineage tracing of Wt1-expressing cells in adult mouse intestine. Adult mice with the $Wt1^{CreERT2/+}$; $Rosa26^{cofetti/LacZ}$ reporter system were analysed 2 weeks and 6 months after tamoxifen administration, respectively. Random segments (8 per animal; group size n = 3) of intestine were analysed by confocal microscopy after short fixation to eliminate peristalsis. Random Z-stacks were recorded and the number of cells scored into two groups: individual cells for all three reporters (as defined by no contact to same-colour cells) and cell clones (as defined by contact to same-colour cells). A, B. Exemplary images of intestine segments from short-term (A) and long-term chase experiments (B). The image of the short-term experiment shows one 2-cell clone (blue, 2c), while that of the long-term experiment shows one 6-cell clone (red, 6c), one 3-cell clone (yellow, 3c) and two 2-cell clones (blue and yellow, 2c). Individual non-clonal cells were found as well. C. Grouped Scatter Graph showing the ratios of clonal versus non-clonal cell numbers from individual animals including the standard deviation of the mean (group size n = 3). Statistical analysis was performed using unpaired multiple t-tests with Holm-Šídák multiple comparisons correction for 2-cell- (adjusted p value = 0.026), 3-cell- and 4+-cell-clone ratios (both adjusted p value = 0.086). D. Table summarizing the scores for clonal and non-clonal cells including ratio for individual animals of short- and long-term chase and pooled totals. Scale bars are 100 μm (A, B).

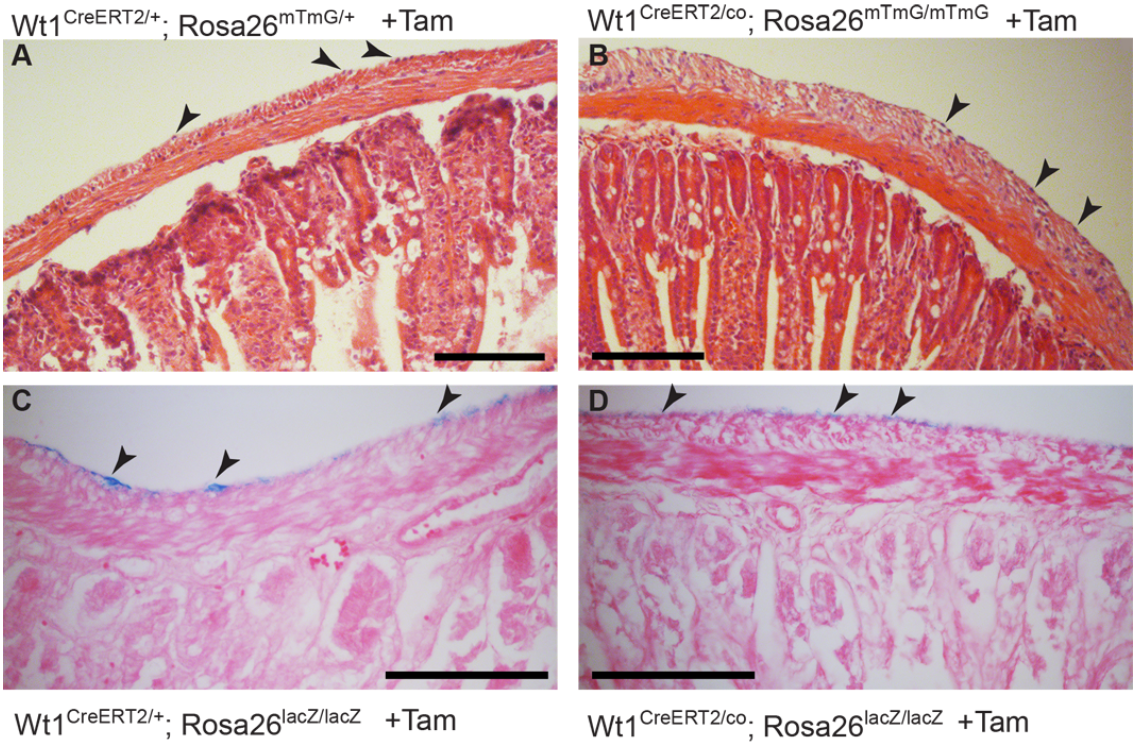

Supplementary Figure S6. Ablation of Wt1 in adult intestine. Tamoxifen was given to mice carrying either the $Wt1^{CreERT2/co}$ alleles, or the $Wt1^{CreERT2/+}$ alleles, for 5 consecutive days. Mice were sacrificed on day 10 and the intestines harvested and XGal stained and/or directly processed for histology (H&E or Eosin counter stain). After tamoxifen, mice with and without the conditional Wt1 allele showed normal architecture of the intestinal wall, with mesothelial cells present as visualised by nuclear Haematoxylin staining (A, B) or by XGal staining (C, D). Scale bars, 100 μm (A-D).

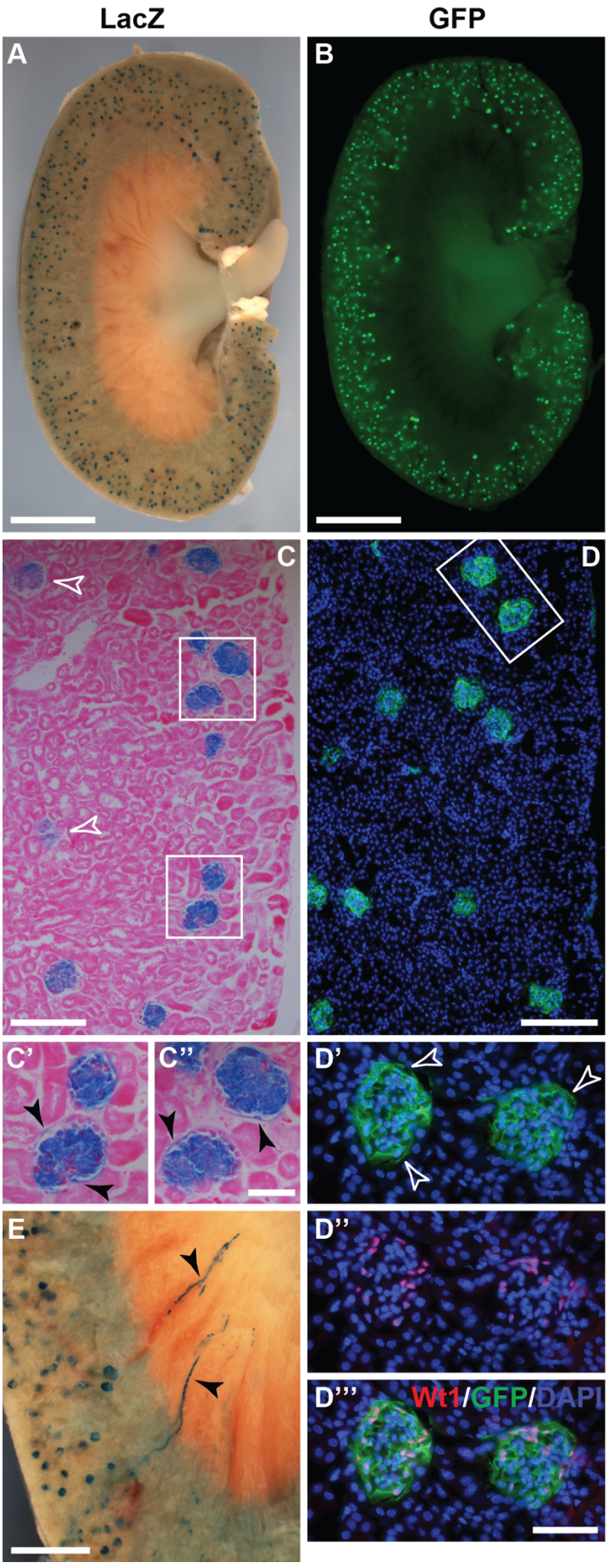

Supplementary Figure S7: Whole mount and histological analysis of adult kidney after lineage tracing of Wt1-expressing cells. Adult mice with either the $Wt1^{CreERT2/+}$;$Rosa26^{LacZ/LacZ}$ or the $Wt1^{CreERT2/+}$; $Rosa26^{mTmG/mTmG}$ reporter system were analysed 2-4 weeks after tamoxifen administration. A, B. In kidney whole mounts (sagittal halves), labelled cells expressing LacZ or GFP were found in the glomeruli. C. Eosin-counterstained sagittal paraffin sections showing LacZ-expression in the glomeruli of the kidney (open arrowheads pointing to glomeruli showing weaker XGal staining due to reduced penetration of staining reagents into tissue). C', C''. LacZ-expressing cells are also detected in the parietal epithelial layer of the Bowman Capsule (filled arrowheads). D. Immunofluorescence in frozen sagittal kidney sections revealed GFP-expressing cells in the glomeruli. D'-D'''. GFP-labelled cells co-expressed Wt1 (D', GFP and DAPI; D'', Wt1 and DAPI; D''', merged). E. In rare cases, LacZ-expressing cells were found in tubular structures reaching into the renal medulla (filled arrowheads). Scale bars, 2 mm (A, B), 300 μm (C, D), 100 μm (C', C'', D'-D'''), 700 μm (E).

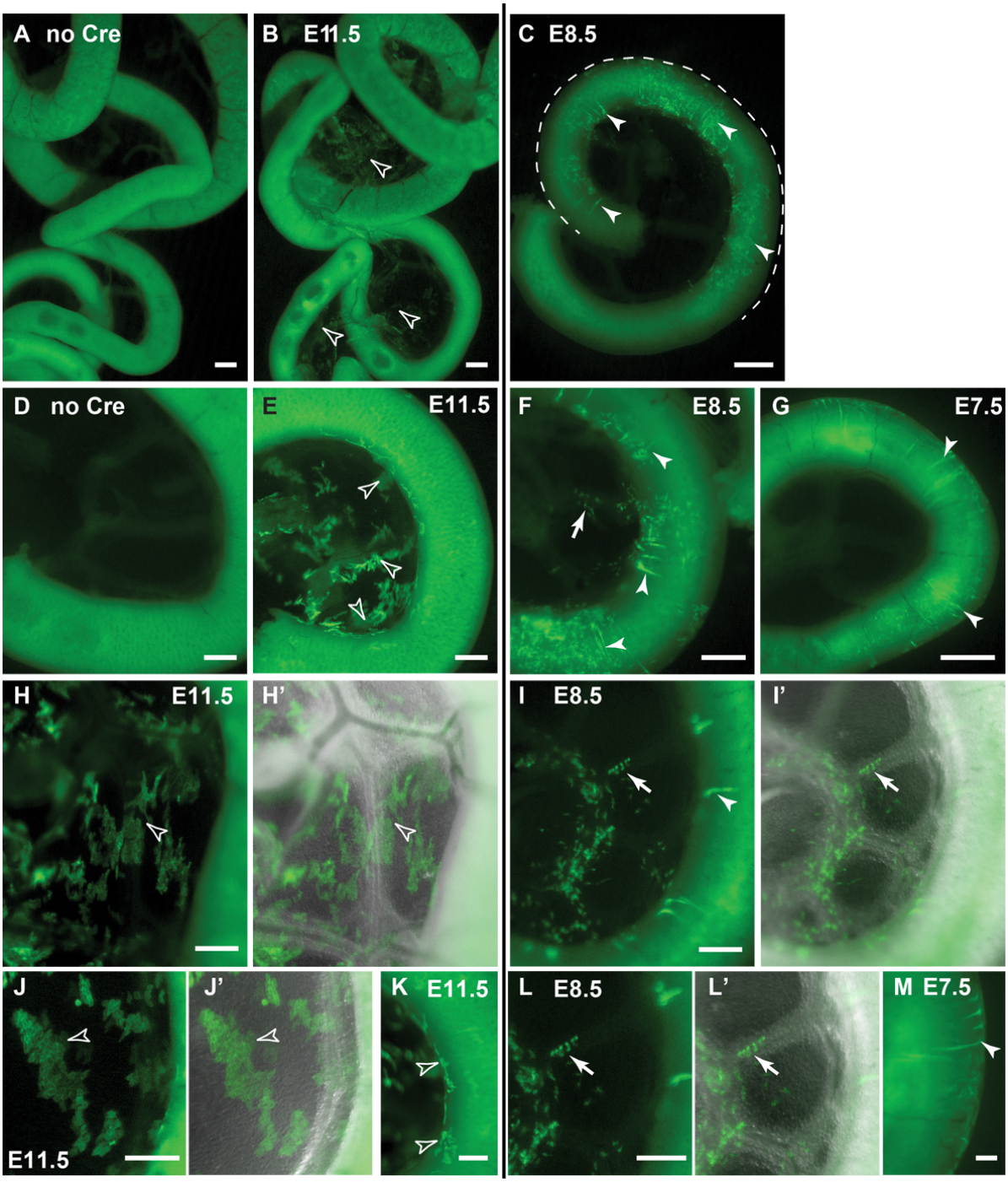

Supplementary Figure S8. Wt1 lineage in embryos using the Rosa^{mTmG} reporter. Analysis of embryos after time mating of Wt1$^{CreERT2/+}$; Rosa26$^{mTmG/mTmG}$ males with CD1 females and tamoxifen at E11.5, E8.5 or E7.5. A, D. In pups negative for the CreERT2 modification and after tamoxifen at E11.5 and analysis at E19.5, no GFP-positive cells were observed. B. In CreERT2-positive littermates, GFP-expressing cells were observed within the mesentery (open arrowheads) along the entire lengths of the small intestine. E, H, J, K. This included patches of GFP+ stained cells over the intestine, and across the mesentery (open arrowheads). C. When tamoxifen was given at E8.5 and

embryos analysed at E17.5, GFP-expressing cells were found in restricted segments (stippled line) along the intestinal tract only, and comprised circular visceral smooth muscle (arrowhead). F, I, L. Besides in visceral smooth muscle (arrowheads), GFP expression was also found in cells surrounding mesenteric vessels (arrows). G, M. GFP-positive cells in the visceral smooth muscle were also observed after tamoxifen at E7.5 and analysis at E18.5 (arrowheads). Scale bars, 500 μm (A, B, C, G), 300 μm (D, E, F), 200 μm (H, I, J, K, L, M).

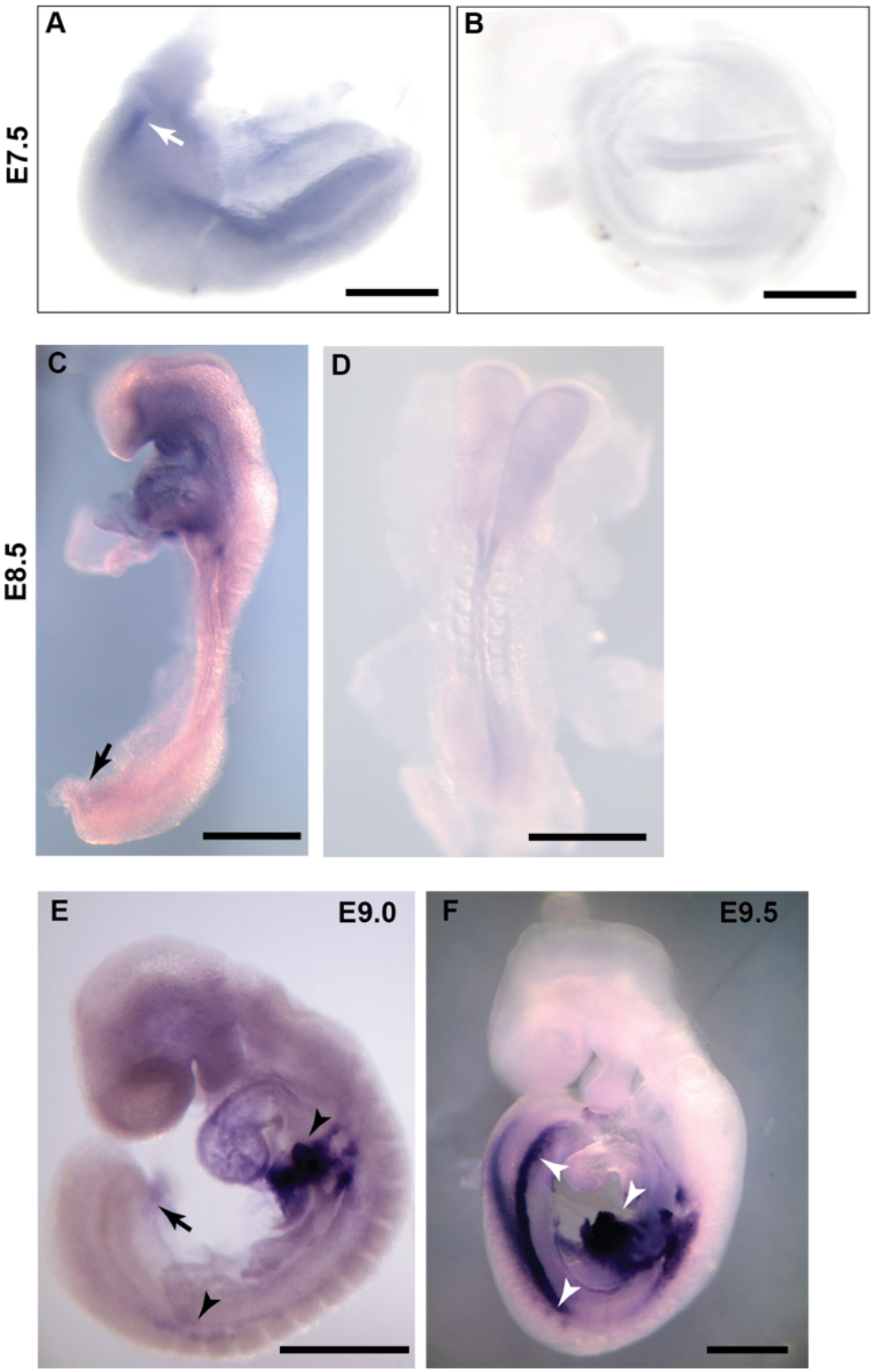

Supplementary Figure S9. In situ hybridisation for *Wt1* between E7.5 and E9.5. A. C. At E7.5 and E8.5, there are generally low levels of diffuse signal detectable across the embryo. At E8.5, the head and heart regions showed a slightly stronger signal, and in both stages we detected a specific faint signal at the posterior of embryo in the primitive streak region (arrow). B, D. Hybridisation with the sense control at these stages yielded no signal at all. E. In the E9.0 embryo, there was a

faint line of expression in the forming urogenital ridge, while strong expression could be detected in the pro-epicardium (arrowheads). At the posterior end of the embryo in the region of the primitive streak, a faint signal was also detectable (arrow). F. At E9.5, the urogenital ridge and pro-epicardium showed strong expression of Wt1 (arrowheads). Scale bars, 200 μm (A, B), 500 μm (C, D, E, F).

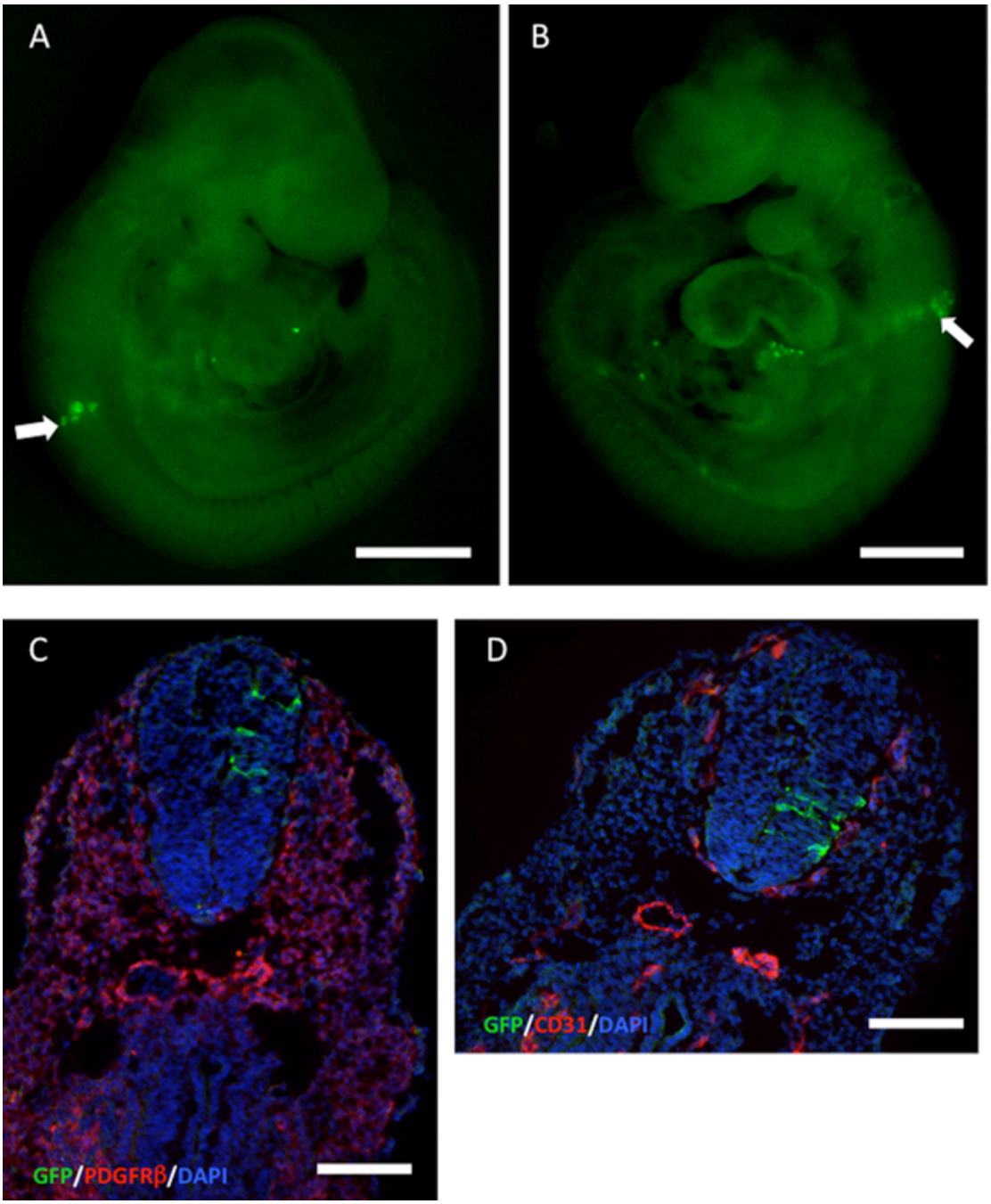

Supplementary Figure S10. Contribution of Wt1-expressing cells to the neural tube after tamoxifen at E7.5. A, B. In four E9.5 embryos out of three litters, cells were identified in the neural tube at the level of the heart (arrows). C, D. This observation was confirmed by immunofluorescence staining of sections through this region. Scale bars, 500 μm (A, B), 100 μm (C, D).

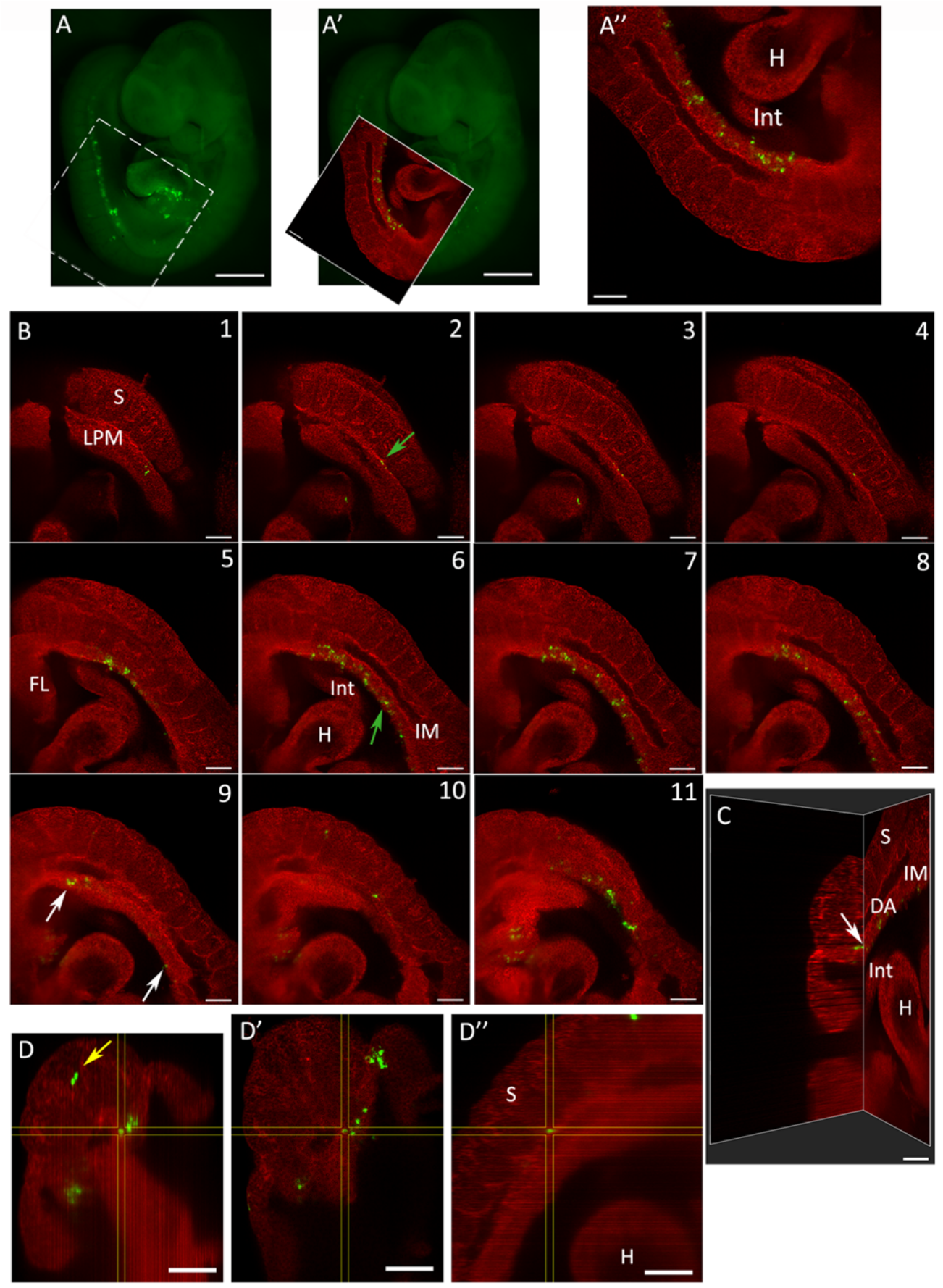

Supplementary Figure S11. Light sheet microscopy analysis of Wt1 lineage at E9.5 after tamoxifen dosing at E8.5. A, A'. Overview images combining dissecting microscopic (DM) and

light sheet microscopic images to demonstrate the specific area of an embryo imaged in the light sheet microscope (LSM). A''. The light microscope image analysis includes part of the heart, the forelimb, and the trunk of the body. (DM) Scale bars, 500 μm (A, A', for DM), 200 μm (A', A'', for LSM). B. Eleven selected slices of light sheet microscopy z-stacks of embryo shown in A, sagittally from lateral towards midline, demonstrate patches of GFP-positive cells in the lateral plate and intermediate mesoderm (green arrows) as well as the tissue close to the dorsal aorta and mesentery (white arrows). Images were generated by the Slice View function in IMARIS software. The membrane-bound dTomato appears in red (561 nm) to illustrate the body structure. Lateral plate mesoderm (LPM), intermediate mesoderm (IM), forelimb (FL), intestine (Int), Somites (S). Scale bars, 200 μm. C. GFP-positive cells were detected in the mesentery (arrow), located between the dorsal aorta (DA) and the intestine (Int). The Ortho Slicer tool in IMARIS was used to visualise the respective cells in the 3D z-stack of the embryo. Scale bar, 200 μm. D. Dorsal (D), frontal (D') and lateral views (D'') of selected GFP-positive cell located in the mesentery. Yellow arrow points to GFP-labelled cells in the neural tube. Size of the crosshair is 30 μm in all three axes X, Y and Z. Scale bars, 200 μm.

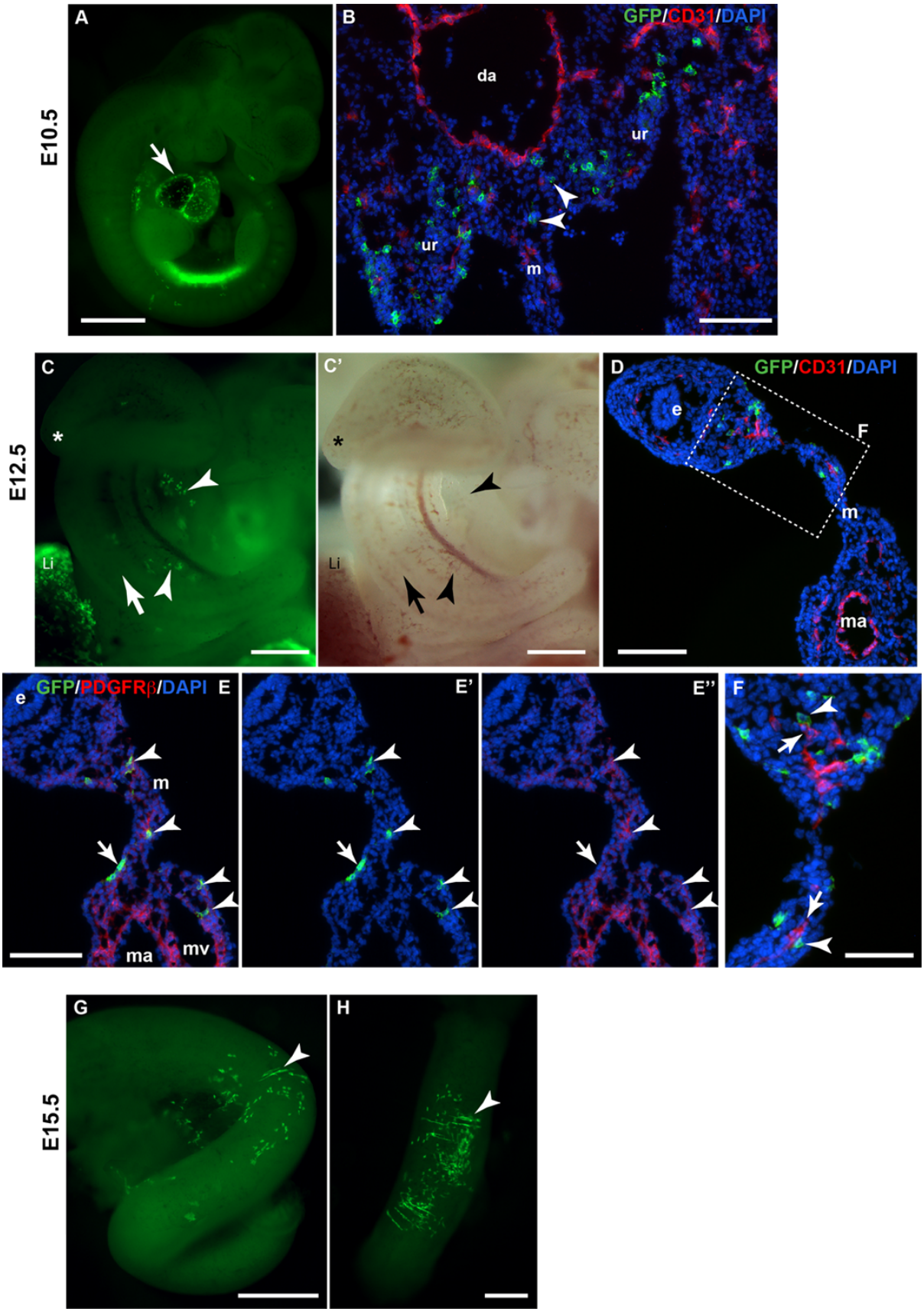

Supplementary Figure S12. Wt1 lineage from E8.5 onwards revealed contribution to the mesentery near developing vasculature and into visceral smooth muscle. A, B. Analysis of embryos at E10.5 after tamoxifen at E8.5. The distribution of GFP-expressing cells throughout the

embryo was increased, and the heart was clearly outlined with GFP-positive cells (A, arrow). By immunofluorescence, GFP-positive cells were detected in the region between dorsal aorta (da), urogenital ridge (ur) and mesentery (m) (B, arrowheads). C-F. Analysis of embryos at E12.5 after tamoxifen at E8.5. GFP-positive cells (arrowheads) were found within the mesentery of the developing intestinal tract (C, C', arrow; star depicts caecum). Note the abundant GFP fluorescence in the liver (Li). Immunofluorescence for CD31 and GFP on sections through this region showed GFP-positive cells within the mesentery and in the intestinal wall, near the developing microvascular plexus (D). Higher magnification (F) reveals that GFP-positive cells (arrowheads) are often close to endothelial cells (arrows) of the vascular plexus in the intestinal wall and mesentery. Immunofluorescence for PDGFRβ and GFP on neighbouring sections revealed that only GFP-positive cells within the intestinal wall mesenchyme and mesentery co-express PDGFRβ (arrowheads), but not few mesothelial GFP-positive cells (E-E'', arrow). G, H. Analysis of embryos at E15.5 after tamoxifen at E8.5. GFP-positive circular visceral smooth muscle fibres (arrowheads) were detectable in the small intestine (G) and colon (H). e, endoderm, m, mesentery, ma, mesenteric artery, mv, mesenteric vein. Scale bars, 1000 μm (A), 100 μm (B, D, E-E''), 300 μm (C, C'), 50 μm (F), 500 μm (G, H).

Stage at Tamoxifen	Stage at analysis	Lineage marker	Number of embryos analysed	Mesothelium (mesentery, intestine)	Vascular smooth muscle	Visceral smooth muscle
E14.5	E19.5	LacZ	3	++	-	-
E14.5	E18.5	LacZ	9	++	-	-
E13.5	E17.5	LacZ	3	+++	-	-
E12.5	E19.5	LacZ	1	+++	-	-
E11.5	E17.5	LacZ	3	++	-	-
E11.5	E19.5	LacZ	6	++	-	-
E11.5	E19.5	mTmG	2	++	-	-
E10.5	E18.5	LacZ	9	+	-	-
E9.5	E19.5	LacZ	2	+	+	+
E9.5	E17.5	LacZ	1	+	-	-
E8.5	E18.5	LacZ	2	+	+	+
E8.5	E18.5	LacZ	2	+	+	-
E8.5	E17.5	mTmG	6	+	+	+
E7.5	E19.5	LacZ	2	-*	+	-
E7.5	E18.5	LacZ	4	-*	+	+
E7.5	E18.5	mTmG	10	-*	+	+

Supplementary Table 1. Summary of lineage analysis in embryos. '-' indicates no labelled cells; '+', '++', '+++' indicate different levels of coverage of labelled cells; '-*' indicate scattered distribution of undetermined individual labelled cells in the mesentery.